Reply to Referee #3

Thank you very much for your valuable comments. In the future we will examine the sustained wind speed by using different criteria to figure out which averaging time is more adequate to represent maximum sustained wind in a TC.

The description of grid resolution and time step in our experiment are listed as following:

Domain	Grid resolution	Time step
D1	27km	30.00s
D2	9km	10.00s
D3	3km	3.33s
D4	1km	1.11s
D5	333.3m	0.37s
D6	111.1m	0.12s
D7	37.03m	0.04s

Minor corrections:

1. P5, line 108, "When the horizontal resolution was decreased... should read "When the horizontal resolution was increased…"

2. P9, line 198, "…wind size…" should be "…window size…"

We have revised the manuscript and the above errors have been corrected.

Reply to Referee #4

Some comments and suggestions are provided below:

Line 92-94: "Such strong turbulence was also observed in Hurricane Isabel (2003) and Felix (2007) at different altitudes (Aberson et al. 2006; Aberson et al .2007)". It is better to list the exact altitudes of this "different altitudes" to make sure these are related to TC BL turbulence.

The extreme updraft (~25 m/s) and horizontal wind (107 m/s) was found at about 1.5 km in Hurricane Isabel (2003). The extreme updraft (~ 31 m/s) was found at about 3km in Hurricane Felix (2007). These extreme updrafts are consistent with the analysis by Stern et al. (2016).

The sentence has rewritten as: Such strong turbulence was also observed in Hurricanes Isabel (2003) below 3-km (Aberson et al. 2006; Aberson et al. 2017).

2. Line 94-96: "Understanding of the structure and evolution of the ... severe turbulence." This sentence doesn't match the logic. The reason to understanding of this small structure turbulence should be it is important for determining storm intensity, it should not be hard to observe. Using numerical simulation is because it is hard to observe.

The sentence has been revised.

3. Line 132-145: The finest resolution of horizontal resolution of this simulation is 37 meters, while the vertical resolution is only 75 levels. This concerns as the ratio of horizontal resolution and the vertical resolution could play a big role in the 3D simulations.

We understand your concern. The vertical resolution in the innermost domain is relatively coarse compared to the horizontal spacing of 37 m. We did not run experiments to examine the sensitivity to the vertical resolution because of the limit of the computation resource. In fact, we attempted to increase the vertical resolution, but the model cannot run on Tianhe-2 computer. For this reason, we conducted the LES-111 experiment (111.1m horizontal resolution) with 12 vertical levels below 1km. In LES-111 experiment, the vertical resolution and horizontal resolution are comparable in the TC boundary layer. The near-surface linear coherent structures and tornado-scale vortex (TSV) simulated in LES-111 are similar to those in the LES-37 experiment. In the revised manuscript, we have added a brief description about the issue.

4. Line 156-157: "we will focus on the hourly output from 26h to 36h." Since this is tornado scale feature and the horizontal resolution reaches 37m, hourly output is too coarse and would miss some features. Suggest taking a more aggressive evaluation of output of the order of minutes (at least 15 minutes).

You are right. The hourly output is to coarse to analyze the tornado scale features. For this reason, we stored the 3-second model output to examine the evolution of the simulated TSVs. Since the 3-second output does not contain the thermodynamic variables, we need rerun the experiment for further analysis.

5. It is better to indicate the red dots as tornado-scale vortices in Fig.2a in figure caption.

The figure caption has been rewritten.

Reply to Referee #5

General Comments:

In this study, the authors use WRF-LES to simulate a quasi-idealized tropical cyclone (in the environment of a real TC), for the purpose of investigating tornado-scale vortices. They find such vortices along the inner eyewall, concentrated in the left-of-shear region where convection is enhanced by the environmental vertical wind shear. Large horizontal gradients of wind speed are found in association with strong updrafts, and from the perturbation wind structure, the authors identify distinct vortices. The authors also argue that the tornado-scale vortices are related to horizontal roll vortices, and they suggest that the vortices may be related to the local large vertical wind shear that is present in the low-level eyewall.

Overall, this is an interesting study that contributes to our knowledge of intense small-scale vortices that are believed to be prevalent within the low-level eyewall of intense tropical cyclones. I have a number of minor scientific comments that are mostly related to requests for clarifications, but also include some areas where I'm not quite convinced that the authors' analysis demonstrates what is claimed. I also have a few more significant concerns. First, I think it is possible that the use of a moving average to define the reference state for wind speed may result in an exaggeration of the gradients in the perturbation winds, and that the azimuthal mean (or azimuthal-mean + low-wavenumber flow) may be a better choice for this analysis. Second, a study (Stern and Bryan 2018) has recently been published, that also used LES to examine these eyewall vortices, and so I think (in revision) that this current study should include some discussion of how their results may relate to those of Stern and Bryan (though I recognize that the authors submitted their manuscript just prior to the appearance online of the earlier study, so I don't mean this as a critique of this manuscript). Finally, it seems that a major result of this study is the finding that the eyewall vortices are related to pre-existing horizontal roll vortices within the boundary layer at and outside of the eyewall. I'm not fully convinced this is the case (though it may be), as the authors haven't really objectively defined the horizontal roll vortices that they see, and the existence of an updraft/downdraft couplet in the tornado-scale vortex isn't itself (in my view) necessarily a horizontal roll vortex (also see minor comments #25-26). Following revisions, I think that this study can be a nice contribution to the literature.

Specific Major Comments:

A. *Use of a moving average to define the reference state*

I think it may be problematic to use the 8-km moving average for calculating perturbation winds. This choice results in the much weaker tangential winds *within the eye influencing the perturbation winds in the tornado-scale vortices, and vice versa. For example, in Fig. 3b, the perturbation flow within the eye is apparently anticyclonic, as the mean winds are much stronger than the local flow (because they include a region of the eyewall). This results in an exaggerated characterization of the vortices, because the mean radial gradients are influencing the perturbation structure. I think a better choice would be to use the azimuthal mean (at a given radius) to define the perturbation winds. I see that the authors have examined something similar to this and they stated that they found similar results to their choice of the moving average. Still, I think the azimuthal mean is a more appropriate choice than the moving average.*

Thank you for your suggestion. Based on the numerical study conducted by Green et al. (2015), we chose the 8-km moving average for calculating perturbation winds. We have checked the results of 2 different methods for calculation perturbation winds. One is the 8-km moving average filter method, and the other is low-wavenumber (azimuthal-mean + wavenumber1-3) flow filer method. From the attached figure (Fig. A2), we can see an exaggerated characterization of the vortices indeed exist inside the eyewall by using the 8-km moving average, but the two different methods have little effect on the perturbation wind field associated with the tornado-scale vortex. We have mentioned this in the revised manuscript.

B. *Discussion of other recent related studies*

With respect to observations of extreme local wind speeds and updrafts that are believed to be related to small-scale vortices, I think it would be worthwhile to discuss the recent study of Stern et al. (2016), who examined extreme updrafts and wind speeds observed by dropsondes. Also, Stern and Bryan (2018) very recently published a study using LES to investigate similar features as to what the authors examine in this manuscript. This was probably not available to the authors at the time that they submitted their manuscript, but given the similarity in some of the goals and methods of these studies, I think it would be worthwhile for the authors to add some discussion of how their results may relate to those of Stern and Bryan (2018).

Thank you for providing the latest references. We added the discussion on the study of Stern et al. (2016) and Stern and Bryan (2018) in the revised manuscript.

C. *Results that are not shown*

There are a fairly large number of results that the authors refer to that aren't actually shown (given in minor comments below). This can be ok, but they need to make clear when a claim isn't explicitly shown by a figure. Also, these *results that aren't shown probably shouldn't be included in the abstract (e.g., that the in nearly all vortices, there is also a broad downdraft).*

In the revised manuscript, we have explicitly indicated the figures that are not shown.

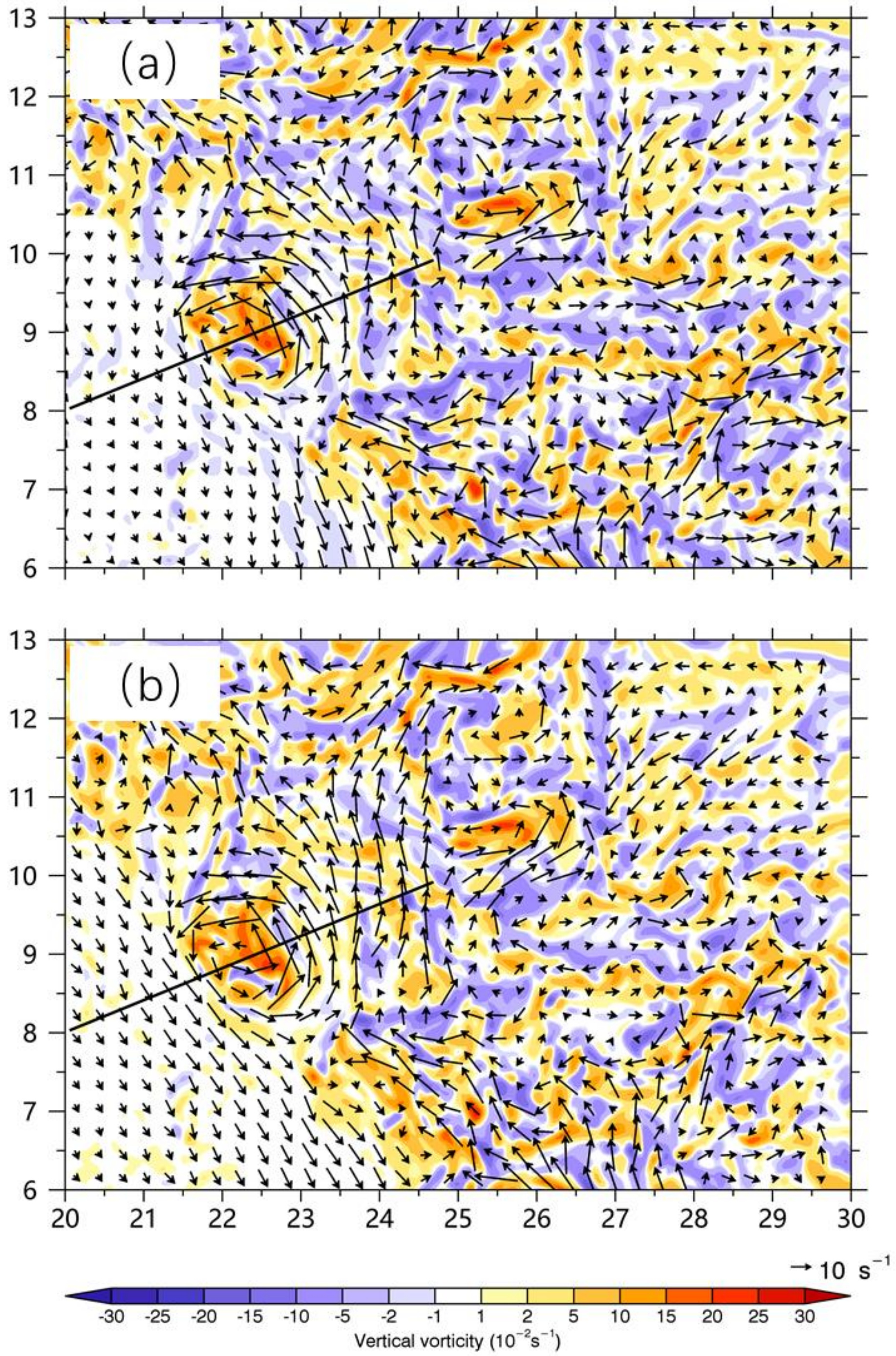

Figure A2 Comparison of the perturbation wind field as shown in Fig. 3b from (a) the result of low-wavenumber (azimuthal-mean + wavenumber 1-3) flow filer method and (b) the result of the 8-km moving average filter.

Specific Minor Comments:

1. *P5 l117*

   "may be responsible for TC intensification" is too strong, I suggest changing to "may contribute to". It also might be a good idea to note here (I see it is mentioned later) that other subsequent studies (such as Bryan and Rotunno 2009) have found that this mechanism is unimportant for intensification.

   Changed.

2. P6 l126-131

   It's a bit unclear why a real case is chosen, but without any evaluation of the simulation in comparison to the observed storm. I'm guessing that the goal here is to examine a realistically sheared storm (and this may be easier to do in the real-case framework), but not to reproduce the evolution or structure of a specific real typhoon. This is ok, but the reasoning here should be made clearer. I note that Typhoon Matsa was not particularly intense, only an estimated 90 kt peak intensity, whereas it appears that the simulated storm here is stronger.

   We used the real case because we want to make the simulated TC evolves in a realistic environment. The typhoon was first simulated in Wu and Chen (2016) without using the LES. For convenience, we used the initial and boundary conditions in this study. As you mentioned, we found that the occurrence of the simulated tornado-scale vortices is closely associated with the environmental shear.

   You are right. The estimated intensity of Typhoon Matsa was not very intense. It is interesting to note that its intensity is close to the azimuthal mean maximum wind speed of the simulated TC although the simulated gust winds are much stronger. It is possible that the simulated TC intensity is stronger than the real typhoon. It is also possible that the maximum sustained wind speed was missed in the observation.

3. *P6 l159-160*

   The authors state that they output 3-s data for a 22-min period at t=29 h. This output is only used briefly on page 11 (with no figures shown), and so I think it would be better to move the description here to be part of the discussion of where it is used on p11.

   Done.

4. *P8 l172-173*

   Note that the persistence of the open eyewall isn't shown.

We only show the simulated radar reflectivity in Fig. 2. In the revised statement, we explicitly mention the other figures are not shown.

5. *P8 l178*

   The shear given here is 5.2 m/s, but the figure caption gives 7.0 m/s.

   The shear is 7.0 m/s. Corrected.

6. *P8 l181*

   The period here is stated to be 11 hours, but above it is given as 10 h. Also, not that the RMW range is not shown.

   Corrected.

7. *P8 l187*

   Clarify that you are referring to the TC-scale shear-induced convective asymmetry here, not local enhancement of reflectivity around the tornado-scale vortices.

   Clarified.

8. *P9 l202 and Fig. 3b*

   The figure is somewhat confusing, because the labels for the identified vortices are not found where the actual features are. It would be good to add a dot/circle (or some other symbol) to indicate the specific locations. Also, I think it would be better to describe the convention for numbering the vortices here (where they are first introduced), rather than later when referring to Table 1.

   The figure is revised.

9. *P9 l209-211, p10 l213-221*

   The authors refer to the features examined here as "tornado-scale" vortices, and they discuss this in the context of the studies of Aberson et al. (2006), Aberson et al. (2017), and Marks et al. (2008). But these prior studies did not refer to the features as "tornado-scale", and so this could be somewhat misleading. The more recent study of Wurman and Kosiba (2018) did use this terminology, and I think it can be an appropriate choice. But the authors should clarify how previous studies viewed these features.

   This has been clarified in the revised manuscript.

10. *P10 l217*

    Why is there a height threshold used in the definition here?

    In this study, we limit our discussion in the TC boundary.

11. *P10 l218*

These thresholds are somewhat arbitrary. Also, we don't really know that these are vortices simply from the vorticity threshold, as a region of high vorticity isn't necessarily a vortex.

These thresholds are based on the observation. We examined all of the identified TSVs and found that all of the TSVs are associated with strong horizontal circulation.

12. *P10 l231-232*

I agree that these vortices may be responsible for the strongest wind gusts in TCs, and this is also consistent with the results shown in Stern and Bryan (2018).
The reference is cited in the revised manuscript.

13. *P10 l227-238*

I'm of the belief that the small-scale vortices probably don't have a substantial effect on the overall intensity evolution. However, I don't think the analyses in this study can really answer this question one way or the other, since we don't know how this simulation would have evolved in the absence of these features.

You are right. Our statement is based on the occurrence of the simulated TSVs. As shown in Figure 1, the azimuthal-mean maximum wind speed does not show any jump at 27 h, when there are 10 identified tornado-scale vortices.

14. *P11 l245-246*

I note that this relationship between the vertical wind shear orientation and the spatial distribution of extreme updrafts is consistent with what Stern et al. (2016) found from dropsonde observations in many storms.

The reference has been cited in the revised manuscript.

15. *P11 l246-251*

It could be good to discuss Stern and Bryan (2018) and Wurman and Kosiba (2018) here, as these studies both estimated the period for which these vortices/updrafts could be tracked (and with similar time periods as the authors have found).

Thank you for your suggestion. We have revised the description.

16. *P11 l254-255*

I think it would be good to make clear that the authors are not directly identifying "vortices", but rather are identifying strong updrafts that are collocated with strong vorticity, and they are inferring that these are likely vortices (aside from the specific example vortices that they more directly identify).

We have examined all of the 24 TSVs and all of them are associated with strong horizontal circulation.

17. *P11 l257-258*

That the updrafts/vortices are often found inward of the mean RMW is somewhat consistent with Stern and Bryan (2018), though in their study, they found that the strongest updrafts tended to occur more nearly at the RMW.

We have cited this paper in the revised manuscript.

18. *P11 l258*

Clarify that you are referring to the w=20 m/s threshold, not the w=15 m/s threshold that has also been examined in this study.

Clarified.

19. *P12 l260-261*

Note that this result is not shown.

Specified.

20. *P12 l271*

Please clarify what is meant by "using the smoothed fields". In what manner is the smoothing done?

We chose the 8-km moving average for calculating perturbation winds. It has been clarified in the revised manuscript.

21. *P12 l271*

Please define the Richardson number.

Added.

22. *P12 l274*

It would be helpful for the authors to more clearly explain why they are examining the Richardson number, what they expect it to tell them, and why they believe it should be related to the existence of these vortices. I see that the authors do so somewhat at the end of this paragraph, but I think it would be good to include this reasoning here where they introduce their analysis.

We have included the expression and more information about Ri in this revision.

23. *P13 l293-294*

I'm not sure what this sentence ("The altitudes of the maximum vertical motions generally increase when the inflow layer deepens outward") means. Perhaps the authors are saying that the height of the features tends to be greater when they are found at larger radii?

You are right. The sentence has been revised.

24. Section 6

It's a bit confusing to have the vortices split into categories without first defining what the categories are. I think the distinctions should be brought up at the beginning of the section, along with information on how specifically the vortices are assigned to a category (is it subjective?), and a discussion of the physical reasoning for these classifications.

You are right. In this study, we subjectively split the vortices into three categories based on its vertical structure, especially in terms of its vertical extension, stratification and near-surface wind jump.

25. *P14 l312-313*

In my opinion, it is hard to tell if the features discussed here are indeed "closely associated with horizontal rolls". Is there any more objective evidence the authors can provide that can better demonstrate this claim?

The horizontal roll is indicated in the new Fig. 6b and Fig. 6c.

26. *P14 l318*

It seems that the authors are concluding that these are roll vortices because there is a updraft/downdraft couplet, and so this implies a transverse circulation and horizontal vorticity. But I don't think this is really the same thing as what is traditionally referred to as a horizontal roll vortex, which generally have an elongated quasi-linear region of weak updrafts/downdrafts. These eyewall vortices will naturally have local updraft/downdraft couplets and large horizontal vorticity, but I don't think this makes them necessarily related to horizontal roll vortices.

Previous studies suggest that the near surface quasi-linear coherent structures are associated with horizontal roll vortices. A typical tornado-scale vortex contains an updraft/downdraft couplet and the updraft in tornado-scale vortex are stronger than in horizontal roll vortices.

27. *P14 l323-324*

In my view, we don't actually know whether the high thetae layer is an indication of transport from the eye. There is high thetae further outward as well in this cross section, so the elevated layer of high thetae does not have to have originated within the eye, although it may have. I think a trajectory analysis is necessary to have confidence on the origin of this air mass.

The sentence has been removed.

28. *P15 l329-331*

It isn't clear to me why/how the downward motion at 500 m is responsible for the high thetae layer. It also is unclear to me why the low thetae layer near the surface should have lower thetae because it is in inflow. It's true that the mean radial gradient tends to be negative (and so mean radial advection tends to yield a negative tendency), but this is generally outweighed by other tendencies (such as surface fluxes).

The sentence has been removed.

29. *P15 l332-333*

Again, I don't think we can know from the analysis here that the high thetae eye air is entrained into the eyewall.

You are right. The related sentence has been revised.

30. *P15 l342-343*

It looks to me that "~65 m/s" should be "~60 m/s", and that "~90 m/s" should be "~95 m/s".

Corrected.

31. *P15 l345*

It isn't clear to me why the downward motion is "consistent" with the "strong wind speed jumps". What is the relationship here? I'm guessing that the authors are implying that strong wind gusts could be caused by vertical advection of higher momentum from above.

You are right.

32. *P16 l360-362*

Is the structure described here for this particular feature believed to be generally true for other such features? It's unclear if there is a robust signature here, as the authors are showing a single example.

The feature is common for tornado-scale vortices in the category. Tornado-scale vortices in the third category mainly occur in the statically stable stratification.

33. *P17 l377-378*

I think it is important to acknowledge here that this definition is somewhat arbitrary, and to reiterate that the frequency of these inferred vortices is very sensitive to the thresholds of this definition.

You are right. We have revised the sentence.

34. *P17 1387*

Here, the authors refer to updrafts stronger than 15 m/s, but their definition given above is for 20 m/s.

Corrected.

35. *P17 1390*

That the updraft is generally associated with a downdraft is not shown.

We explicitly mention figures that are not shown. The updraft and downdraft couplet can be seen in Fig. 6b in the revised manuscript.

36. *Fig. 1*

Make the caption clearer by changing "instantaneous and azimuthal maximum" to "maximum instantaneous and azimuthal-mean".

Corrected.

37. *Fig. 2*

The red dots in 2a aren't defined in the caption. Change "solid circles" to "black circles". Give the height at which the RMW is evaluated here. Insert ", respectively" after "and the radius of maximum wind". Remove "(27h)".

Corrected and added.

38. *Fig. 6*

The "vertical slice" doesn't look exactly vertical to me. Please clarify if it is "nearly" vertical".

Corrected.

39. *Fig. 7*

Please clarify if this cross section is purely in the radial dimension (as opposed to projecting onto the azimuthal dimension as well).

This cross section is in the radial dimension. We have revised the description in our manuscript.

40. *Fig. 9*

Please clarify if the vertical velocity shown here is also a perturbation quantity.

Yes. It is a perturbation quantity.

Technical Corrections:

1. *P2 140*
   "the favorable location" is vague and somewhat confusing. I suggest "the location along the inner edge of the eyewall", or something similar.

   Changed.

2. *P3 166*
   "by now" should be "for now".

   Corrected.

3. *P5 1109*
   "f" should be italicized.

   Corrected.

4. *P6 1134 and elsewhere*
   When expressing the lengths of a grid, the units should be "km", not "km2".

   Corrected.

5. *P6 1134*
   Insert "grid" before "spacing".

   Corrected.

6. *P6 1136*
   "dimentional" should be "dimensional".

   Corrected.

7. *P6 1142*
   Insert "for" after "except".

   Added.

8. *P7 1145*
   Insert "of" after "temperature".

   Added.

9. P7 1160
   Use "29 h" instead of "the 30th hour".

   Corrected.

10. *P7 1162*
    "northern north west" should be "north northwest".

Corrected.

11. *P7 1163-166*

"instantaneous and azimuthal maximum" should be "maximum instantaneous and azimuthal mean", with "maximum" presumably applying to both metrics. The following sentence "The instantaneous output…" can be removed, as it is redundant.

Corrected.

12. *P8 1167, l169*

I think it would be better to put the smaller number first for these ranges.

Corrected.

13. *P8 1176*

Insert "is" after "shear".

Added.

14. *P8 1183*

"France" should be "Frances".

Corrected.

15. *P9 1194*

"filed" should be "field.

Corrected.

16. *P9 1198*

"wind" should be "window".

Corrected.

17. *P9 1209*

Aberson et al. (2016) should be Aberson et al. (2017).

Corrected.

18. *P10 1233*

Insert "some" before "previous".

Added.

19. P10 1235

"Montegomery" should be "Montgomery".

Corrected.

20. *P10 1235*

"azimuthal" should be "azimuthal-mean"

Corrected.

21. *P12 1272*

    Insert "vortex" after "scale".

    Corrected.

22. *P12 1274-275*

    Stern et al. (2016) is cited here, but it doesn't appear in the list of references.

    Added.

23. P14 1305

    Move "inward" from end of sentence to right after "kilometers".

    Corrected.

24. *P14 1318*

    "frank" is a typo here. I think that the authors mean "flank". Also, "rolling" should be "roll" (also where it is used elsewhere).

    Corrected.

25. *P15 1327*

    Replace "To the right" with "Outward".

    Corrected.

26. *P15 1328*

    Change "the category" to "this category", and insert "of vortices" after "category".

    Corrected.

27. *P15 1328*

    It's ambiguous which feature "the lower-altitude high thetae layer" refers to. Please clarify.

    The sentence has been rewritten.

28. *P15 1329*

    Change "does not" to "is not".

    Corrected.

29. *P15 1337*

    I think that the authors may mean Fig. 8a and not Fig. 8b. Also, I think they may mean Fig. 3b and not Fig. 2b.

    Corrected.

30. *P16 1359*

    "Figures 10a" should be "Fig. 10a".

    Corrected.

31. *P16 1367*

Insert "with" after "associated". Insert "the" before "complicated".

Added.

32. *P17 1371*

    Change "nesting" to "nested".

    Corrected.

33. *P17 1382*

    There is an extra period after "layer".

    Corrected.

34. *Fig. 4*

    "500-km" should be "500-m".

    Corrected.

35. Fig. 8

    Fig. 8b has "400 m", but the caption says "500 m".

    Corrected.

36. Fig. 10

    The last sentence of the caption is a duplicate.

    Deleted.

Reply to Referee #2

This paper describes the characteristics of relatively intense tornado-scale vortices in a high-resolution numerical simulation of a mature tropical cyclone under environmental conditions resembling those of Typhoon Matsa (2005). It is found that the simulated vortices have locations and basic properties that are broadly consistent with limited observations. An effort is made to classify the vortices into 3 distinct categories. In my view, the article is well organized and provides useful information that is adequately summarized in the abstract and section 7. Moreover, I did not catch any obvious mistakes of major consequence. On the other hand, I was somewhat disappointed not to see a rigorous analysis of the generation and decay of a tornado-scale vortex belonging to any of the 3 categories. High-resolution TC simulations showing tornado-scale vortices are not unprecedented [e.g., Stern and Bryan 2014], and it seems to me that the most interesting scientific questions pertain to the formation and decay mechanisms. Below are some minor comments that might be worth considering before official publication.

We absolutely agree with you that this manuscript does not include a rigorous analysis of the generation and decay of the tornado-scale vortex. As we mentioned in the manuscript, the model output is regularly stored at 1-h intervals, and a few variables during a 22-min period from the 30th hour are also stored at 3-s intervals. In this study, we mainly used 1-hour outputs to check the structures of tornado-scale vortices. We think that considerable analysis is needed to understand the mechanisms for the generation and decay of the tornado-scale vortex. We plan to rerun the experiment by adding more variables in the 3-s output and investigate the mechanisms for the generation and decay of the tornado-scale vortex in the future. We have added some discussions in the revised manuscript.

1. The paper cites an earlier study suggesting that grid-spacing less than 100 m is necessary for simulating the development of tornado-scale vortices. However, it is not entirely clear to me that simulating the 1-2 km structures of interest requires 37-m horizontal grid spacing, especially since the vertical grid spacing is(apparently)of order 100 m in the boundary layer. A brief comment on what happens to the tornado-scale vortices when the finest horizontal grid is removed in the present numerical experiment might be worthwhile.

Our experiment contains 12 vertical levels below 1 km. We also conducted an experiment with the resolution of 111 m in the innermost domain. In the experiment, the vertical resolution and horizontal resolution are comparable in TC boundary layer. The tornado-scale vortex (TSV) mentioned in observations can also be found in the experiment. In the attached figure, we can see a simulated TSV in the experiment, similar to the TSV in Figure 6. The maximum vertical motion is 21.3 m s^{-1} at 500 m and the maximum relative vertical vorticity is 0.11 s^{-1}. In the revised manuscript, we have added a brief description about the issue.

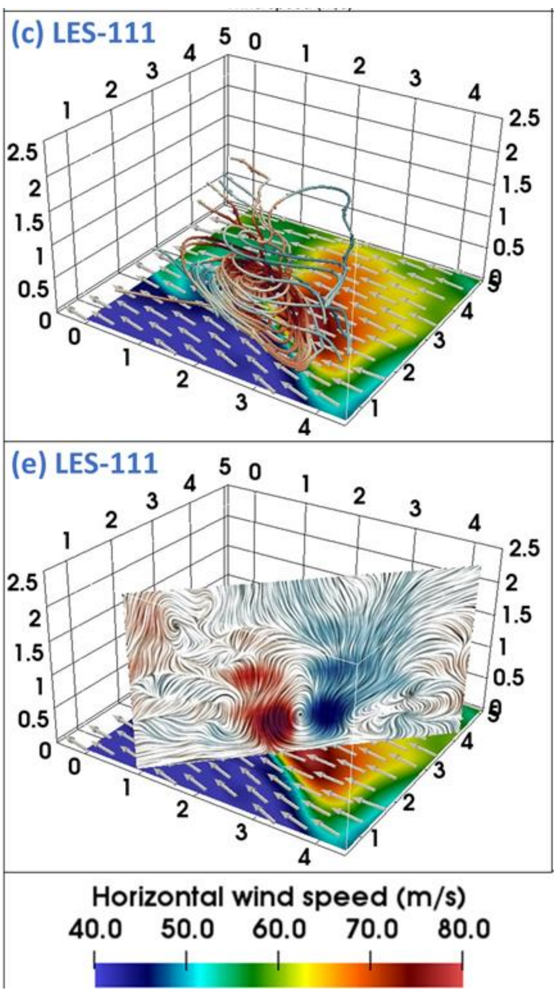

Fig. A1 A simulated TSV in the LES-111 experiment. The description of the figure is the same as Fig. 6 in the manuscript, except for LES-111 experiment.

2. There is a recent LES study by Ito et al. [Scientific Reports, 7.1, 3798 (2017)] that addresses the variation of roll structure with location in a TC boundary layer. Perhaps the authors should to try to connect the aforementioned study to theirs.

Thank you for providing the reference. We have introduced the research conducted by Ito et al. (2017) in the Introduction.

3. Since this article pertains to coherent structures having large horizontal components of relative vorticity, it might be a good idea to specify upfront that the term "relative vorticity" in this paper (presumably) refers to the vertical relative vorticity.

This is a good idea. We have done this in the revised manuscript.

4. Lines 170-171: In my view, it seems a little awkward to introduce tornado-scale vortices as small-scale features that are distinct from horizontal rolls, but later show that they incorporate horizontal rolls (in some sense). That said, I am not sure that any changes need to be made in response to the preceding comment.

In this manuscript, we focus mostly the tornado-scale vortices and the calculated vorticity is the vertical component of relative vorticity. The simulated tornado-scale vortices are distinct from horizontal rolls because the strong updrafts are always accompanied by strong horizontal circulations.

5. Lines 256-258: This statement (added after the first review) needs to be rewritten. To begin with, the statement fails to clarify whether the azimuthally averaged wind speed is an azimuthal average of the total horizontal wind speed or of the tangential (azimuthal) velocity. Of lesser importance, "are directly" should be "are obtained directly", and there should probably be a comma after "time-averaging".

Thank you. The statement has been revised.

6. Line 374: To facilitate quantitative comparison with future studies, I think that it might be worthwhile to more precisely define the Richardson number (with an equation).

We have added some statement on Richardson number. The gradient Richardson number, Ri, has largely been used as a criterion for assessing the stability of stratified shear flow. It is defined by

$$R_i = \frac{N^2}{S^2} \qquad (1)$$

$N^2 = g\frac{\partial \ln \theta_e}{\partial z}$ is the square of Brunt–Väisälä frequency and $S^2 = (\frac{\partial u}{\partial z})^2 + (\frac{\partial v}{\partial z})^2$ is the square of vertical shear of the horizontal velocity, g is the gravity acceleration, θ_e is the equivalent potential temperature, u is the zonal wind speed and v is the meridional wind speed.

7. Lines 426-428: The wording suggests (to me) that the cited studies definitively showed that the wind speed bands are connected to vertical momentum transport by the rolls, but such an interpretation is challenged by the final sentence of the paragraph. I would consider revising the paragraph so as not to mislead the reader upfront.

The sentence has been revised.

8. Line 130: I suggest changing "the similar features as revealed with the limited observational data" to "features similar to those revealed with limited observational data".

The sentence has been rewritten as you suggest.

9. Lines 156-159: This section of the paragraph tries to say too much in one sentence.

The sentence has been rewritten as you suggest.

10. Line 275: I believe that "France" should be "Frances".

Corrected. Thank you!

11. Line 290: "wind size" should be "window size".

Corrected.

12. Line 325: I would change "the mesovortices" to "mesovortices".

Corrected.

13. Line 339: I might remove "consecutive" or change it to "continuous".

Corrected.

14. Lone 350: "close to RMW" should be "close to the RMW".

Corrected.

15. Line 364: "tornado-scale" should be "tornado-scale vortex".

Corrected.

16. Line 404: I would change "Besides" to "In addition".

Changed.

17. Line 410: Should "frank" be "flank"?

Corrected.

18. Line 425: I might change "entrained" to "locally entrained".

Changed.

19. Line 459: "associated strong turbulence" should be "associated with strong turbulence".

Corrected.

20. Lines 463-465: "nesting grids" should be "nested grids"; "shows the similar features as revealed with the limited observations" should be something like "shows features similar to those revealed with limited observations"; "favorable" should probably be "favored".

Thank you. Corrected.

21. Lines 478-480: These sentences seem largely redundant with the preceding paragraph.

We have deleted some sentences in the preceding paragraph.

Reply to Referee # 1

This manuscript documents the small-scale vortices in the tropical cyclone boundary layer found in a two-way nested WRF-LES set up using the large-scale conditions of a real typhoon. The results are interesting and the presentation is quite clear. I have only a few minor comments about the model setup and interpretation of results.

Minor corrections:

1. The 100-m vertical resolution is relatively coarse for adequately resolving structures like the high theta_e layers shown in Fig. 7b. It is also coarse compared to the 37m horizontal resolution. A higher vertical resolution is also desirable for capturing the strength and scale of the horizontal roll vortices mentioned by the authors (Fig. 3a). Have the authors done any sensitivity tests to examine the impact of vertical resolution on the structure and distribution of the small-scale vortices focused on in the work?

We agree with you that the vertical resolution in the innermost domain is relatively coarse compared to the horizontal spacing of 37 m. We did not run experiments to examine the sensitivity to the vertical resolution because of the limit of the computation resource. In fact, we attempted to increase the vertical resolution, but the model cannot run on Tianhe-2 computer. For this reason, we conducted the LES-111 experiment (111.1m horizontal resolution) with 12 vertical levels below 1km. In LES-111 experiment, the vertical resolution and horizontal resolution are comparable in the TC boundary layer. The near-surface linear coherent structures and tornado-scale vortex (TSV) simulated in LES-111 are similar to those in the LES-37 experiment. In the revised manuscript, we have added a brief description about the issue.

2. I couldn't quite infer the exact connection between the "quasi-linear bands" and what is shown in Fig. 8 (paragraph starting on Line 334). Are the authors implying that the wind speed horizontal variability associated with the quasi-linear features could explain in part the wind speed jump associated with the "tornado-scale vortices"? Please be more explicit.

Previous studies suggested that the quasi-linear bands are associated with the horizontal rolls in the TC boundary. Our simulation shows that the simulated tornado-scale vortices are closely associated with horizontal rolls inside the RMW. The enhanced vertical motion increases the upward and downward momentum transports (Fig. 7a), amplifying the horizontal gradient of the near-surface wind speed (Fig. 8b). Therefore, the wind speed horizontal variability associated with the quasi-linear features could explain in part the wind speed jump associated with the tornado-scale vortices. The wind speed jump associated with tornado-scale vortices are clear in Fig. 8, but some tornado-scale vortices are not associated with pronounced near-surface wind speed jump. We have made it more explicit in the revised manuscript.

3. By categorizing the vortices into 3 groups, are the authors suggesting that they are generated/maintained by different physical mechanisms? Could they simply represent different phases in the life cycle of these coherent structures?

You are right. In this manuscript we did not focus on the mechanisms for tornado-scale vortex generation and maintenance. We think that considerable analysis is needed to understand the mechanisms. While strong vertical and horizontal wind shear inside eyewall may be important for the development of the tornado-scale vortices, we suggest that the three categories of tornado-scale vortices are associated with different hydrostatic stratification.

We used the 3-second model output to examine the evolution of the simulated tornado-scale vortices. It seems that the beginning of most simulated tornado-scale vortices is associated with horizontal rolls. Since the 3-second output does not contain the thermodynamic variables, we cannot examine the hydrostatic stratification. At this time we are not sure that the three categories represent different phases in the life cycle of these coherent structures. We have made it more explicit in the revised manuscript.

Tornado-Scale Vortices in the Tropical Cyclone Boundary Layer: Numerical Simulation with WRF-LES Framework

Liguang Wu[1,2], Qingyuan Liu[1] and Yubing Li[1]

[1]Pacific Typhoon Research Center and Key Laboratory of Meteorological Disaster of Ministry of Education, Nanjing University of Information Science and Technology, Nanjing, China

[2]Department of Atmospheric and Oceanic Sciences and Institute of Atmospheric Sciences, Fudan University, Shanghai, China

December 20, 2018

Revised for *Atmos. Chem. Phys.*

Corresponding author address: Dr. Liguang Wu
Pacific Typhoon Research Center
Nanjing University of Information Science and Technology, Nanjing, Jiangsu 210044
E-mail: liguang@nuist.edu.cn

Abstract

The tornado-scale vortex in the tropical cyclone (TC) boundary layer (TCBL) has been observed in intense hurricanes and the associated intense turbulence poses a severe threat to the manned research aircraft when it penetrates hurricane eyewalls at a lower altitude. In this study, a numerical experiment in which a TC evolves in a large-scale background over the western North Pacific is conducted using the Advanced Weather Research and Forecast (WRF) model by incorporating the large eddy simulation (LES) technique. The simulated tornado-scale vortex shows features similar to those revealed with limited observational data, including the updraft/downdraft couplet, the sudden jump of wind speeds, the location along the inner edge of the eyewall, and the small horizontal scale. It is suggested that the WRF-LES framework can successfully simulate the tornado-scale vortex with the grids at the resolution of 37 m that cover the TC eye and eyewall.

The simulated tornado-scale vortex is a cyclonic circulation with a small horizontal scale of ~1 km in the TCBL. It is accompanied by strong updrafts (more than 15 m s^{-1}) and large vertical components of relative vorticity (larger than 0.2 s^{-1}). The tornado-scale vortex favorably occurs at the inner edge of the enhanced eyewall convection or rainband within the saturated, high-θ_e layer, mostly below the altitude of 2 km. Nearly in all the simulated tornado-scale vortices, the narrow intense updraft is coupled with the relatively broad downdraft, constituting one or two updraft/downdraft couplets or horizontal rolling vortices, as observed by the research aircraft. The presence of the tornado-scale vortex also leads to significant gradients in the near surface wind speed and wind gusts.

1. Introduction

Tropical cyclones (TCs) pose a severe risk to life and property in TC-prone areas and the risk will increase due to the rapidly rising coastal population and buildings (Pielke et al. 2008; Zhang et al. 2009). One of the major TC threats is damaging winds. Uneven damage patterns often show horizontal scales ranging from a few hundred meters to several kilometers (Wakimoto and Black 1994; Wurman and Kosiba 2018), suggesting that TC threats are associated with both sustained winds and gusts. The latter are believed to result from small-scale coherent structures in the TC boundary layer (Wurman and Winslow 1998; Morrison et al. 2005; Lorsolo et al. 2008; Kosiba et al. 2013; Kosiba and Wurman 2014). The small-scale coherent structures may have significant implications for the vertical transport of energy in TCs and thus TC intensity and structure (Zhu 2008; Rotunno et al. 2009; Zhu et al. 2013; Green and Zhang 2014, 2015; Gao et al. 2017). While understanding of the coherent structure is very important for mitigating TC damage and understanding of TC intensity and structure changes, for now direct in situ observation and remote sensing measurements can only provide very limited information.

In the TC boundary layer (TCBL), observational analyses suggest that horizontal streamwise roll vortices prevail with sub-kilometer to multi-kilometer wavelengths (Wurman and Winslow 1998; Katsaros et al. 2002; Morrison et al. 2005; Lorsolo et al. 2008; Ellis and Businger 2010; Foster, 2013). Studies found that the rolls can result from the inflection point instability of the horizontal wind profiles in the TCBL (Foster 2005; Gao and Ginis 2014) and have significant influences on the vertical transport of energy in TCs (Zhu 2008; Rotunno et al. 2009; Zhu et al. 2013; Green and Zhang 2014, 2015; Gao et al. 2017). The TCBL is known to play a critical role in transporting energy and controlling TC intensity (Braun and Tao 2000; Rotunno et al. 2009; Smith and Montgomery 2010; Bryan 2012; Zhu et al. 2013; Green and Zhang 2015).

Another important small-scale feature is the so-called eyewall vorticity maximum (EVM) (Marks et al. 2008) or tornado-scale vortices in the TCBL (Wurman and Kosiba 2018; Wu et al. 2018). So far, our understanding is mainly from a few observational analyses based on limited data collected during the research aircraft penetration of hurricane eyewalls. A WP-3D research aircraft from National Oceanic and Atmospheric Administration (NOAA) encountered three strong updraft-downdraft couplets within one minute while penetrating the eyewall of category 5 Hurricane Hugo (1989) at 450-m altitude (Marks et al. 2008). The severe turbulence caused the failure of one of the four engines and the people aboard were at a severe risk. The aircraft finally escaped with the help of a U. S. Air Force reconnaissance WC-130 aircraft, which found a safe way out through the eyewall on the northeast side of Hugo. Since then the aircraft mission has been prohibited in the boundary layer of the TC eyewall. Later analysis indicated that the dangerous turbulence was associated with a tornado-scale vortex, which is comparable to a weak tornado in terms of its diameter of about 1 km and the estimated peak cyclonic vorticity of 0.125 s^{-1} (Marks et al. 2008). Such strong turbulence was also observed in Hurricanes Isabel (2003) and Felix (2007) below 3 km (Aberson et al. 2006; Aberson et al. 2017). So far, little is known about the structure and evolution of the tornado-scale vortex.

With advances in numerical models and computational capability, the large eddy simulation (LES) technique has been incorporated into the Advanced Weather Research and Forecast (WRF) model (Mirocha et al. 2010) and an increasing number of TC simulations have been conducted with horizontal grid spacing less than 1 km (Zhu 2008; Rotunno et al. 2009; Bryan et al. 2014; Stern and Bryan 2014; Rotunno and Bryan 2014; Green and Zhang 2015). In LES, the energy-producing scales of 3-dimensional (3D) atmospheric turbulence in the planetary boundary layer (PBL) are explicitly resolved, while the smaller-scale portion of the turbulence is parameterized (Mirocha et al. 2010). Effort has been made to simulate the structure of the TC PBL eddies and the associated influence on TC intensity. Zhu (2008) simulated the structure of the coherent large eddy circulations and the induced vertical transport using the WRF-LES framework with horizontal resolutions of 300 m and 100 m. When the horizontal resolution was increased from 185 to 62 m on the *f*-plane, Rotunno et al. (2009) found a sharp increase in randomly distributed small-scale turbulent eddies, while 1-minute mean TC intensity began to decrease. Green and Zhang (2015) performed several 6-hour one-way simulations of Hurricane Katrina (2005) without a boundary layer parameterization (horizontal resolutions of 333, 200, and 111 m). Rotunno et al. (2009) and Green and Zhang (2015) suggest that the horizontal resolution should be below 100 m to simulate the development of 3D turbulent eddies in TCBL. Ito et al. (2017) found that the near-surface coherent structures can be successfully simulated by using the horizontal resolution of 70 m, which appear to be caused by an inflection-point instability of both radial and tangential winds.

It is clear that understanding of the tornado-scale vortex would enhance the safety of flights into very intense TCs. In addition, the tornado-scale vortex may contribute to TC intensification by mixing the high-entropy air in the eye into the eyewall (Persing and Montgomery 2003; Montgomery et al. 2006; Aberson et al. 2006) and track fluctuations

(Marks et al. 2008; Aberson et al. 2017). By simulating the tornado-scale vortex in the TCBL, this study will particularly focus on the spatial distribution of the occurrence of the tornado-scale vortex and the features of its 3D structures.

2. The numerical experiment

In this study the numerical simulation is conducted using version 3.2.1 of the WRF model. Following Wu and Chen (2016), two steps were taken to construct the initial conditions for the numerical experiment. A symmetric vortex was first spun up without the environmental flow on an *f*-plane for 18 hours and then the vortex was embedded in the large-scale background of Typhoon Matsa (2005) from 0000 UTC 5 August to 1200 UTC 6 August. The large-scale environment was derived from the National Centers for Environmental Prediction (NCEP) Final (FNL) Operational Global Analysis data with resolution of 1.0° × 1.0° using a 20-day low-pass Lanczos filter (Duchon 1979).

The spun-up vortex is initially located at the center of Typhoon Matsa (25.4°N, 123.0°E). The outermost domain centered at 30.0°N, 132.5°E covers an area of 6210×6210 km with a horizontal grid spacing of 27 km. The numerical experiment is designed with six two-way interactive domains embedded in the 27-km resolution domain to simulate energetic 3-dimensional turbulent eddies in the TC eyewall and their influence on the TC vortex, mesoscale rainbands and convective clouds. The horizontal spacing decreases by a factor of 3 with the domain level. The corresponding horizontal resolutions are 9 km, 3 km, 1 km, 1/3 km (333 m), 1/9 km (~111 m) and 1/27 km (~37 m) and the numbers of their grid meshes are 230×210, 432×399, 333×333, 501×501, 1351×1351, and 2431×2431, respectively. The innermost domain covers the inner region of the simulated TC (90×90 km^2), including the eye and eyewall. Except for the 27-km and 9-km resolution domains, the other domains move with the TC. The model consists of 75 vertical levels (19 levels below 2 km) with a top of 50 hPa and is run over the open ocean with a constant sea surface temperature of 29ºC.

The physics options used in the simulation are as follows. The Kain-Fritsch cumulus parameterization scheme and the WRF single-moment 3-class scheme are used in the outermost domain (Kain and Fritsch 1993). The WRF 6-class scheme is selected in the nested domains with no cumulus parameterization scheme (Hong and Lim 2006). The Rapid Radiative Transfer Model (RRTM) and the Dudhia shortwave radiation scheme are used for calculating long-wave radiation and shortwave radiation (Mlawer et al. 1997; Dudhia 1989). The LES technique is used in the sub-kilometer domains (Mirocha et al. 2010) and the Yonsei University scheme is adopted for PBL parameterization in the other domains (Noh et al. 2003).

The model is run for 36 hours and the 1/9-km-resolution and 1/27-km-resolution domains are activated at 24 h. In the following analysis, we will focus on the hourly output from 26 h to 36 h. The TC center is determined with a variational approach in which it is located until the maximum azimuthal-mean tangential wind speed is obtained (Wu et al. 2006).

3. The simulated small-scale features

The simulated TC takes a north northwest track (figure not shown). Figure 1 shows its intensity in terms of the maximum instantaneous and azimuthally averaged wind speeds at 10 m in the 1/27 km-resolution domain. The instantaneous winds are obtained directly from the model output without any time averaging. The azimuthal wind speed is the wind speed averaged azimuthally with respect to the TC center. The instantaneous maximum wind speed fluctuates between 61.8 m s^{-1} and 76.6 m s^{-1} during the 12-hour period, while the fluctuations in the azimuthal maximum wind speed is relatively small, ranging from 43.5 m s^{-1} to 48.8 m s^{-1}. In particular, the TC maintains the azimuthal mean maximum wind speed of ~45 m s^{-1} after the innermost domain has been activated for two hours.

Figure 2a shows the simulated 500-m radar reflectivity at 27 h, indicating that the eyewall is open to the south of the TC center. We examine the radar reflectivity field and find that the opened eyewall persists during the 11-hour period (figure not shown). In addition, the location of the enhanced convection relative to the TC center is generally steady. It is well known that the eyewall asymmetry is associated with the vertical shear of the environmental flow (Frank and Ritchie 2001, Braun and Wu 2007). In this study the vertical wind shear is calculated as the difference of wind vectors between 200 hPa and 850 hPa within a radius of 300 km. As shown in the figure, the mean shear is 7.0 m s^{-1} to the southeast over the 11-hour period. In agreement with the previous studies, the enhanced eyewall reflectivity is generally observed in the downshear left side. There are relatively small changes in the RMW during the 11-hour period, ranging from 28.2 km to 30.7 km at 500 m.

Using the fine-scale dual Doppler data in the right front quadrant and eye of Hurricane Frances (2004) as it made landfall on Florida, Kosiba and Wurman (2014) found linear coherent structures with a wavelength of 400-500 m near the surface. Figure 2b shows the simulated near-surface (10 m) wind speeds in the inner region at 27 h. The instantaneous wind speed is dominated by quasi-linear coherent structures in the eyewall region. The intense instantaneous wind speeds coincide with the TC-scale shear-induced enhanced eyewall convection shown in Figure 2a. In order to show clearly the quasi-linear feature, we plot the instantaneous wind speed in an area of 7×10 km^2 at this time (Fig. 3a). The small area is located in the eyewall to the east of the TC center (Fig. 2b). The streaks of alternating high and low wind speeds can be clearly seen, which are roughly aligned with the TC-scale flow with an outward angle. We can see that the instantaneous wind speed exhibits large gradients across the quasi-linear structures.

Figure 3b shows the perturbation wind field at 500 m in the small area. The perturbation winds are obtained by subtracting an 8-km moving mean. We compare the perturbation winds with different sizes of the moving window. While the perturbation wind fields are very similar, the wind speeds generally increase with the increasing window size. When the window size is larger than 8 km, there is little change in the perturbation wind speed. The simulated small-scale circulations are similar to those by subtracting the symmetric and wavenumber 1-3 components with respect to the TC center. In the perturbation wind field, we can see two small-scale cyclonic circulations. The most distinct one has a diameter of ~2 km. In the next section, the two cyclones are identified as two tornado-scale vortices (M2701 and M2705). In the study, the simulated tornado-scale vortex is named with four digits. While the first two digits indicate the hours of the simulation, the last two digits is the series number at the same hour. Compared to Figure 3a, the two tornado-scale vortices also correspond to enhanced wind speeds at 10 m.

4. Identification of TSVs

As mentioned in Section 1, analyses of a few real cases in Atlantic intense hurricanes indicate that the tornado-scale vortex is a small-scale feature that occurs in the turbulent TC boundary, with vertical motion and relative vorticity extremes. Aberson et al. (2006)

and Aberson et al. (2017) analyzed the extreme updrafts in Hurricanes Isabel (2003) and Felix (2007) and suggested that the strong updrafts were likely associated with the small scale vortex. The updraft of 25 m s^{-1} in Isabel was detected by a GPS dropwindsonde just below 800 hPa, while the updraft of 31 m s^{-1} in Hurricane Felix (2007) was observed at the flight altitude (~ 3 km). Marks et al. (2008) found that the EVM in Hurricane Hugo (1989) was associated with a maximum vertical motion of 21 m s^{-1} and a maximum vertical relative vorticity of 0.125 s^{-1} at the altitude of 450 m. Based on these studies, a small scale vortex associated with extreme wind speed can be treat as tornado-scale vortex (Wurman and Kosiba 2018; Wu et al. 2018). The tornado-scale vortex in the simulated TC is subjectively defined as a small-scale cyclonic circulation with the diameter of 1-2 km below the altitude of 3 km, containing maximum upward motion larger than 20 m s^{-1} and maximum vertical relative vorticity larger than 0.2 s^{-1}. The grid points that satisfy the thresholds of vertical motion and vertical relative vorticity belong to the same tornado-scale vortex if they are within a distance of 1 km in the horizontal or vertical direction. We detect the tornado-scale vortices using the output at one-hour intervals from 26 h to 36 h. A few variables are also stored at 3-second intervals during a 22-minute period from the 30 h.

There are 24 tornado-scale vortices identified in the 11-hour output (Table 1). There are four tornado-scale vortices with the maximum vertical motion more than 30 m s^{-1} and the maximum vertical component of relative vorticity larger than 0.4 s^{-1}. Except for the two tornado-scale vortices at 36 h, the others occur during 26 h-31 h with 10 cases at 27 h. The lull period is coincident with relatively weaker instantaneous maximum wind speed at 10 m although there is little difference in the azimuthal mean maximum wind speed

(Fig. 1). Examination indicates that the 10-m instantaneous wind speed maximum at 27 h is associated with M2701. It is suggested that the tornado-scale vortex can lead to the strongest wind gust in a TC.

Some previous studies argued that the presence of mesovortices intensifies the TC by mixing the high-entropy air in the eye into the eyewall (Persing and Montgomery 2003; Montgomery et al. 2006; Aberson et al. 2006). As shown in Figure 1, the azimuthal-mean maximum wind speed does not show any jump at 27 h, when there are 10 identified tornado-scale vortices. In the following discussion, we will show that the mixing indeed exists, but its effect on the azimuthal maximum wind speed cannot be detected. It is similar with the conclusion from idealized numerical experiments conducted by Bryan and Rotunno (2009). In fact, the azimuthal maximum wind speed (~45 m s^{-1}) is rather steady during the 11-hour period after the innermost domain has been activated for two hours.

The number of the identified tornado-scale vortices is sensitive to the threshold of vertical motion. If we relax the threshold of maximum vertical motion to 15 m s^{-1}, we can identify 89 tornado-scale vortices during the 11-hour period (Fig. 4a). Nearly all the tornado-scale vortices still occur in the same semicircle of the enhanced eyewall reflectivity. This relationship between the vertical wind shear orientation and the spatial distribution of extreme updrafts is consistent with what Stern et al. (2016) found from dropsonde observations in many storms. In our experiment, a few variables are also stored at 3-second intervals during a 22-minute period from the 30th hour. The duration of the tornado-scale vortex is examined in the 3-second output. The duration is counted as the continuous period during which the maximum vertical motion and vertical relative vorticity are not less than the thresholds. For the thresholds of 20 m s^{-1} in vertical motion and 0.2 s^{-1} in vertical relative vorticity, the mean duration is 40 seconds and the longest is 138 seconds. We can conclude that the identified tornado-scale vortices are not repeatedly counted in the 1-hour output. Besides, the durations of tornado-scale vortices are consistent with the observational and numerical studies (Wurman and Kosiba 2018; Stern and Bryan 2018).

5. Spatial distribution of tornado-scale vortices

Figure 4a shows the location of the maximum vertical motions of the detected tornado-scale vortices including 89 vortices identified with the threshold of maximum vertical motion of 15 m s^{-1}. Different criteria give similar distribution pattern of tornado-scale vortices, thus we just discuss the 24 tornado-scale vortices defined under the threshold of maximum vertical motion of 20 m s^{-1} in the following discussion. The tornado-scale vortices exclusively occur in the semicircle with intense convection from the east to the northwest (Fig. 2a). Nearly all of the identified cases occur in the inward side of the radius of maximum wind (RMW) or close to the RMW (e.g., Stern et al. 2016; Stern and Bryan 2018), with two exceptions that are located outside of the RMW (Fig. 4a). One is M2901, which is 11.8 km from the RMW, and the other is M3601 being 7.3 km from the RMW (Table 1). Close examination indicates that the two tornado-scale vortices occur between two high reflectivity bands (figure not shown).

Although the real tornado-scale vortices were observed by chance, they were also associated with the intense radar reflectivity within the hurricane eyewall and sharp horizontal reflectivity gradients (Aberson et al. 2006, Marks et al. 2008 and Aberson et al. 2016). In agreement with these studies, all of the simulated tornado-scale vortices are associated with sharp horizontal reflectivity gradients and most of them occur in the inner edge of the intense eyewall convection within the RMW. As shown in Figure 2a, all of the 10 cases at 27 h are located in the inner edge of the intense reflectivity. It is suggested that the tornado-scale vortex favorably occurs at the inner edge of the intense eyewall convection.

The gradient Richardson number (Ri) has largely been used as a criterion for assessing the stability of stratified shear flow. It is defined by

$$R_i = \frac{N^2}{S^2} \qquad (1)$$

where $N^2 = g\frac{\partial\, ln\, \theta_e}{\partial z}$ is the square of Brunt–Väisälä frequency, $S^2 = (\frac{\partial u}{\partial z})^2 + (\frac{\partial v}{\partial z})^2$ is the square of vertical shear of the horizontal velocity, g is the gravity acceleration, θ_e is the equivalent potential temperature, u is the zonal wind speed, and v is the meridional wind speed. z is the vertical coordinate. Using the smoothed fields, we also calculate the Richardson number for each tornado-scale vortex (Table 1). It is calculated at each level and then averaged over a layer between 200 m and 800 m within a radius of 1.5 km from the location of the maximum vertical motion. The Richardson number is small, and it is negative for seven cases. As suggested by Stern et al. (2016), the strong updraft is mainly within a kilometer of the surface and it is implausible for buoyancy to be the primary mechanism for vertical acceleration. In Figure 4a, the Richardson number is also plotted, which is averaged over the 11-hour period. We can see that the tornado-scale vortices generally occur in the areas with the Richardson number less than 0.25. It is indicated that the flow in these areas is dynamically unstable and turbulent. The areas coincide with the semicircle of the enhanced eyewall convection. Figure 4b further shows the field of the Richardson number at 27 h. The 10 tornado-scale vortices are all in an environment with the Richardson number less than 0.1. Since the Richardson number is calculated as the ratio of the moist static stability to the vertical wind shear in the TCBL, we speculate that the strong vertical wind shear in the inward side of the intense eyewall convection is an important factor for the development of tornado-scale vortices.

Figure 5 shows the vertical cross sections of tangential wind, radial wind, vertical motion, reflectivity and vertical relative vorticity below 2.5 km, which are averaged in the northeast quadrant over the 11-hour period. Note that the radial locations of M2901 and M3601 are not shown in Figure 5 due to the effect of the limited innermost domain on the calculation of the azimuthal mean. Note that there are relatively small changes in the RMW during the 11-hour period. The maximum vertical motions associated with the tornado-scale vortices are located inside the tilted RMW between the altitudes of 300 m and 1300 m. Most of them (71%) are found between 400 m and 600 m. The height of the maximum vertical motions becomes higher when the inflow layer deepens outward. Figures 5b and 5c further indicate that the tornado-scale vortices are generally found in the region of strong vertical motion averaged over the northeastern quadrant, where the vortices are detected, and large vertical relative vorticity with sharp horizontal reflectivity gradient on the inward side of the eyewall.

6. Tornado-scale vortex structure

Using the high-resolution model output, we can explore the structural features of the simulated tornado-scale vortex. After examination of all of the identified 24 tornado-scale vortices, we find that they can be classified into three categories based on its vertical structure, especially in terms of its vertical extension, stratification and near-surface wind jump.

The first category includes 17 cases, accounting for 71% of the total. Their structural features can be represented by M2701, one of the four strongest tornado-scale vortices, located 4.3 kilometers inward from the 500-m RMW (Table 1). In fact, the four strongest belong to the same category. In this category, nearly all of the maximum vertical motions occur around the altitude of 500 m, except M3001. The maximum vertical motion of M2701 is 31.98 m s^{-1} at the altitude of 400 m, while the maximum vertical relative vorticity of 0.55 s^{-1} occurs at 200 m (Table 1). The 3D structure of the tornado-scale vortex can be clearly demonstrated by the streamlines of perturbation winds near the strong updraft (Fig. 6). The flows curl cyclonically upward from the surface (Fig. 6a). The tornado-scale vortex is manifested by a small-scale circulation extending upward to ~1.5 km. In addition, the tornado-scale vortex is closely associated with updraft/downdraft couplets (Fig. 6b). Fig. 6c shows that the tornado-scale vortex is a complex twisted vortex system. The system has strong horizontal circulation below 1-km and it turns into vertical circulation as the height increases. So it contains both strong horizontal and vertical circulations.

Figure 7 shows the vertical cross section of vertical motion, equivalent potential temperature, and simulated radar reflectivity along the line in Figure 3b for M2701. The inflow from the outward side and the outflow from the eye side converge near the surface to the strong updraft that is below ~1.5 km. The updraft and the downward motion to its radially outward flank constitute a horizontal rolling vortex. On the top of the updraft, there is a layer of the high equivalent potential temperature (θ_e) layer (Fig. 7b). To the eye side of the updraft, there is a high θ_e layer below ~1.5 km. The high θ_e layer tilts upward and extends outward. The large radar reflectivity can be found below the high θ_e layer (Fig. 7c). The intense updraft is located in the inner edge of the large radar reflectivity region. In addition, as suggested by Aberson et al. (2006) and Marks et al. (2008), the strong updraft is within a saturated layer (Fig. 8a), coinciding with high vertical relative vorticity (Fig. 8c).

To the right of the updraft (Fig. 7b), another high θ_e layer can be seen at the altitude of ~500 m. We check other cases in this category of vortices and find that the lower-altitude high θ_e layer is not always present. The downward motion at ~500 m may be responsible for the lower-altitude high θ_e layer. The relatively low θ_e near the surface corresponds to the inflow layer. The high θ_e air meets with the cold inflow air, resulting in relatively lower θ_e in the strong updraft. It is indicated that the high θ_e air in the eye is locally entrained into the TC eyewall.

Some previous studies have shown that the quasi-linear bands are closely associated with the horizontal rolls in the TC boundary layer due to the upward and downward momentum transports (Wurman and Winslow 1998; Katsaros et al. 2002; Morrison et al. 2005; Lorsolo et al. 2008; Ellis and Businger 2010; Foster 2013). To demonstrate the relationship, Figure 8b shows the cross section of winds along the line shown in Figure 3b and the corresponding wind speeds at 10 m and 400 m. The figure clearly shows that the wind speed fluctuations at 10 m are associated with the changes of the vertical motions in Fig. 7a. The wind speed jump (Fig. 8b) is significant across the intense updraft (Fig. 7a). At 10 m, the wind speed suddenly increases from ~30 m s^{-1} to ~60 m s^{-1}. Note that the wind speed jump is larger at 400 m, ranging from ~35 m s^{-1} to ~95 m s^{-1}. Marks et al. (2008) reported that the wind speed at 450-m altitude increased rapidly from <40 m s^{-1} to 89 m s^{-1} in the Hurricane Hugo (1989) when the NOAA research aircraft encountered an EVM. We argue that the superposition of the horizontal cyclonic circulation of the tornado-scale vortices plays an important role in enhancing wind gusts on its radially outward side.

There are three tornado-scale vortices in the second category, including M2706, M2707 and M2708. The structural features can be represented by M2708. In M2708, the maximum vertical motion and vertical relative vorticity occur at 900 m and 800 m, respectively (Table 1). The vertical motion of more than 12 m s^{-1} extends vertically from the near surface to ~2 km (Fig. 9a). In this category, we cannot see the warm air with high θ_e (Fig. 9b) and the strong updraft is located in a statically unstable stratification (Table 1). The wind speed at the altitude of 900 m varies by ~20 m s^{-1} across the updraft, while the wind speed gradient is relatively weak at 10 m (Fig. 9c).

The third category includes four cases: M2600, M2703, M2705 and M3002, in which the updraft occurs in a statically stable stratification (Table 1). Here we use M3002 as an example to show its vertical structure. As shown in Fig. 10a, the updraft is elevated between 0.5 km and 2 km. The maximum vertical motion and relative vorticity are found at the altitude of 1300 m. In this category, a pronounced feature is the deep low θ_e (less than 364 K) layer in the inflow layer (Fig. 10b). As shown in Figure 10c, the gradient of the wind speed at 10 m is not clear while there is a speed jump of ~30 m s^{-1} in the vicinity of the updraft at 1300 m.

Previous studies suggest that the horizontal resolution should be below 100 m to simulate the development of 3D turbulent eddies in TCBL (Rotunno et al. 2009; Green and Zhang 2015). Based on our numerical experiment, the tornado-scale vortex can be successfully simulated with the grids at the resolution of 37 m. It should be noted that we have 12 vertical levels below 1km.Vertical resolution in the innermost domain seems to be relatively coarse compared to the horizontal spacing of 37 m. We also conducted the an experiment with the innermost domain resolution of 111 m. In the experiment, the vertical resolution and horizontal resolution are comparable in TC boundary layer. The tornado-scale vortices can also be found in the experiment. At this time, we are not sure that the three categories represent different phases in the life cycle of these coherent structures, since the 3-second output does not contain the thermodynamic variables, we cannot examine the hydrostatic stratification.

7. Summary

The tornado-scale vortex or EVM in the TCBL has been observed in intense hurricanes and is always associated with strong turbulence. To understand the complicated interactions of the large-scale background flow, TC vortex, mesoscale organization, down to fine-scale turbulent eddies, a numerical experiment in which a TC evolves in a typical large-scale background over the western North Pacific is conducted using the WRF-LES framework with six nested grids. The simulated tornado-scale vortex shows features similar to those revealed with limited observations. It is suggested that the WRF-LES framework can successfully simulate the tornado-scale vortex with the grids at the resolution of 37 m that cover the TC eye and eyewall.

Following Wu et al. (2018), the tornado-scale vortex can be defined as a small-scale cyclonic circulation with the maximum vertical motion not less than 20 m s^{-1} and maximum vertical relative vorticity not less than 0.2 s^{-1}. A total of 24 tornado-scale vortices can be identified in the 11-hour output. Nearly all of them are within or close to the RMW. Most of them occur in the inward side of the intense eyewall convection, mostly below the altitude of 2 km. Tornado-scale vortices are mostly in neutral or stable stratification within the saturated, high-θ_e layer. The tornado-scale vortex generally occurs in the areas with the Richardson number less than 0.25. We speculate that the strong vertical wind shear in the inward side of the intense eyewall convection is an important factor for the development of tornado-scale vortices.

The simulated tornado-scale vortex has a small horizontal scale of 1-2 km in the TCBL. It is accompanied by strong updrafts (more than 20 m s^{-1}) and a cyclonic circulation with large vertical components of relative vorticity (larger than 0.2 s^{-1}). The tornado-scale vortex is closely associated with horizontal rolls. Nearly in all of the simulated tornado-scale vortex cases, the narrow intense updraft is coupled with the relatively broad downdraft (figures not shown), constituting an updraft/downdraft couplet or horizontal rolling vortex, as observed by the research aircraft. Since the tornado-scale vortex is associated with intense updrafts and strong wind gusts, its presence can pose a severe threat to the eyewall penetration of manned research aircraft and the strong wind gusts associated with tornado-scale vortices can pose a severe risk to coastal life and property.

Acknowledgments. We thank Prof. Ping Zhu of Florida International University for aiding with the WRF-LES framework. This research was jointly supported by the

National Basic Research Program of China (2015CB452803), the National Natural Science Foundation of China (41730961, 41675051, 41675009), and Jiangsu Provincial Natural Science Fund Project (BK20150910). The numerical simulation was carried out on the Tianhe Supercomputer, China.

References

Aberson, S. D., Black, M., Montgomery, M. T. and Bell, M.: Hurricane Isabel (2003): New Insights Into the Physics of Intense Storms. Part II: Extreme Localized Wind, *Bull. Amer. Meteor. Soc.*, **87**, 2006.

Aberson, S. D., Zhang, J. A. and Ocasio, K. N.: An Extreme Event in the Eyewall of Hurricane Felix on 2 September 2007, *Mon. Wea. Rev.*, **145**, 2017.

Braun, S. A. and Tao, W.-K.: Sensitivity of High-Resolution Simulations of Hurricane Bob (1991) to Planetary Boundary Layer Parameterizations. *Monthly Weather Review*, **128**, 3941–3961, 2000.

Braun, S. A. and Wu, L.: A Numerical Study of Hurricane Erin (2001). Part II: Shear and the Organization of Eyewall Vertical Motion. *Monthly Weather Review*, **135**, 1179–1194, 2007.

Bryan, G. H., and R. Rotunno: The influence of near-surface, high-entropy air in hurricane eyes on maximum hurricane intensity. *J. Atmos. Sci.*, **66**, 148–158, 2009.

Bryan, G. H.: Effects of surface exchange coefficients and turbulence length scales on the intensity and structure of numerically simulated hurricanes. *Mon. Wea. Rev.*, **140**, 1125–1143, 2012.

Bryan, G. H., Stern, D. P., and Rotunno, R.: A Framework for Studying the Inner Core of Tropical Cyclones Using Large Eddy Simulation, paper presented at 31st Conference on Hurricanes and Tropical Meteorology, *Am. Meteorol. Soc.*, San Diego, Calif, 2014.

Duchon, C. E.: Lanczos filtering in one and two dimensions. *J. Appl. Meteor.*, **18**, 1016–1022, 1979.

Dudhia, J.: Numerical study of convection observed during the winter monsoon experiment using a mesoscale two-dimensional model. *J. Atmos. Sci.*, **46**, 3077-3107, 1989.

Ellis, R. and Businger, S.: Helical Circulations in the Typhoon Boundary Layer. *Journal of Geophysical Research*, **115**, D06205, 2010.

Foster, R.: Why rolls are prevalent in the hurricane boundary layer. *Journal of the atmospheric sciences*, **62**, 2647–2661, 2005.

Foster, R.: Signature of Large Aspect Ratio Roll Vortices in Synthetic Aperture Radar Images of Tropical Cyclones. *Oceanography*, **26**, 58-67, 2013.

Frank, W. M. and Ritchie, E. A.: Effects of vertical wind shear on the intensity and structure of numerically simulated hurricanes. *Mon. Wea. Rev.*, **129**, 2249-2269, 2001.

Gao, K. and Ginis, I.: On the Generation of Roll Vortices due to the Inflection Point Instability of the Hurricane Boundary Layer Flow. *Journal of the Atmospheric Sciences*, **71**, 4292–4307, 2014.

Gao, K., Ginis, I., Doyle, J. D. and Jin, Y.: Effect of Boundary Layer Roll Vortices on the Development of an Axisymmetric Tropical Cyclone. *Journal of the Atmospheric Sciences*, **74**, 2737–2759, 2017.

Green, B. W. and Zhang, F.: Sensitivity of Tropical Cyclone Simulations to Parametric Uncertainties in Air–Sea Fluxes and Implications for Parameter Estimation. *Monthly Weather Review*, **142**, 2290–2308, 2014.

Green, B. W. and Zhang, F.: Numerical simulations of Hurricane Katrina (2005) in the turbulent gray zone, *Journal of Advances in Modeling Earth Systems*, **7**, 142–161, 2015.

Hong, S.–Y. and Lim, J.–O. J.: The WRF single–moment 6–class microphysics scheme (WSM6). *J. Korean Meteor. Soc.*, **42**, 129–151, 2006.

Ito, J., Oizumi T., and Niino H.: Near-surface coherent structures explored by large eddy simulation of entire tropical cyclones. *Sci. Rep.*, **7**, 3798, 2017.

Kain, J. S. and Fritch, J. M.: Convective parameterization for mesoscale models: The Kain–Fritch scheme. *The Representation of Cumulus Convection in Numerical Models*, Meteor. Monogr., Amer. Meteor. Soc., **46**, 165–170, 1993.

Kosiba, K., Wurman, J., Masters, F. J., and Robinson, P.: Mapping of Near-Surface Winds in Hurricane Rita Using Finescale Radar, Anemometer, and Land-Use Data. *Monthly Weather Review*, **141**, 4337–4349, 2013.

Kosiba, K. A. and Wurman, J.: Finescale Dual-Doppler Analysis of Hurricane Boundary Layer Structures in Hurricane Frances (2004) at Landfall. *Monthly Weather Review*, **142**, 1874–1891, 2014.

Lorsolo, S., Schroeder, J. L., Dodge, P., and Marks, F.: An Observational Study of Hurricane Boundary Layer Small-Scale Coherent Structures. *Monthly Weather Review*, **136**, 2871–2893, 2008.

Marks, F. D., Black, P. G., Montgomery, M. T., and Burpee, R. W.: Structure of the Eye and Eyewall of Hurricane Hugo (1989). *Monthly Weather Review*, **136**, 1237–1259,2008.

Mirocha, J. D., Lundquist, J. K., and Kosović, B.: Implementation of a Nonlinear Subfilter Turbulence Stress Model for Large-Eddy Simulation in the Advanced Research WRF Model. *Monthly Weather Review*, **138**, 4212–4228, 2010.

Mlawer, E. J., Taubman, S. J., Brown, P. D., Iacono, M. J., and Clough, S. A.: Radiative transfer for inhomogeneous atmosphere: RRTM, a validated correlated-k model for the longwave. *J. Geophys. Res.*, **102 (D14)**, 16663–16682, 1997.

Montgomery, M. T., Bell, M. M., Aberson, S. D., and Black, M. L.: Hurricane Isabel (2003): New Insights into the Physics of Intense Storms. Part I: Mean Vortex Structure and Maximum Intensity Estimates. *Bull. Amer. Meteor. Soc.*, **87**, 1335–1347, 2006.

Morrison, I., Businger, S., Marks, F., Dodge, P., and Businger, J. A.: An Observational Case for the Prevalence of Roll Vortices in the Hurricane Boundary Layer. *Journal of the atmospheric sciences*, **62**, 2662–2673, 2005.

Noh, Y., Cheon, W. G., Hong, S.-Y. and Raasch, S.: Improvement of the K-profile model for the planetary boundary layer based on large-eddy simulation data. *Bound.-Layer Meteor.*, **107**, 401–427, 2003.

Persing, J. and Montgomery, M. T.: Hurricane Superintensity. *J. Atmos. Sci.*, **60**, 2349–2371, 2003.

Pielke, R. A., Gratz, J., Landsea, C. W., Collins, D., Saunders, M. A., and Musulin, R.: Normalized Hurricane Damage in the United States: 1900–2005. *Natural Hazards Review*, **9**, 29–42, 2008.

Rotunno, R., Chen, Y., Wang, W., Davis, C., Dudhia, J., and Holland, G. J.: Large-Eddy Simulation of an Idealized Tropical Cyclone. *Bulletin of the American Meteorological Society*, **90**, 1783–1788, 2009.

Rotunno, R. and Bryan, G. H.: Effects of resolved turbulence in a large eddy simulation of a hurricane, paper presented at 31st Conference on Hurricanes and Tropical Meteorology, *Am. Meteorol. Soc.*, San Diego, Calif, 2014.

Smith, R. K. and Montgomery, M. T.: Hurricane boundary-layer theory. *Quarterly Journal of the Royal Meteorological Society*, **136**, 1665–1670, 2010.

Stern, D. P. and Bryan, G. H.: The structure and dynamics of coherent vortices in the eyewall boundary layer of tropical cyclones, paper presented at 31st Conference on Hurricanes and Tropical Meteorology, *Am. Meteorol. Soc.*, San Diego, Calif, 2014.

Stern, D. P., Bryan, G. H., and Aberson, S. D.: Extreme Low-Level Updrafts and Wind Speeds Measured by Dropsondes in Tropical Cyclones. *Monthly Weather Review*, **144**, 2177-2204, 2016.

Stern, D. P. and Bryan, G. H.: Using Simulated Dropsondes to Understand Extreme Updrafts and Wind Speeds in Tropical Cyclones. *Monthly Weather Review*, **146**, 3901-3925, 2018.

Wakimoto, R. M. and Black, P. G.: Damage Survey of Hurricane Andrew and Its Relationship to the Eyewall. *Bull. Amer. Meteor. Soc.*, **75**, 189–200, 1994.

Wurman, J. and Winslow, J.: Intense Sub-Kilometer-Scale Boundary Layer Rolls Observed in Hurricane Fran. *Science*, **280**, 555–557, 1998.

Wurman, J. and Kosiba, K.: The Role of Small-Scale vortices in Enhancing Surface Winds and Damage in Hurricane Harvey (2017). *Mon. Wea. Rev.*, **146**, 713-722, 2018.

Wu, L., Liu, Q., and Li, Y.: Prevalence of tornado-scale vortices in the tropical cyclone eyewall. *Proceedings of the National Academy of Sciences,* doi.org/10.1073/pnas.1807217115,2018.

Wu, L., Braun, S. A., Halverson, J., and Heymsfield, G.: A numerical study of Hurricane Erin (2001). Part I: Model verification and storm evolution. *J. Atmos. Sci.*, **63**, 65–86, 2006.

Wu, L. and Chen, X.: Revisiting the steering principle of tropical cyclone motion in a numerical experiment. *Atmos. Chem. Phys.*, **16**, 14925–14936, 2016.

Zhang, Q., Wu, L., and Liu, Q.: Tropical Cyclone Damages in China 1983–2006. *Bull. Amer. Meteor. Soc.*, **90**, 489–495, 2009.

Zhu, P.: Simulation and Parameterization of the Turbulent Transport in the Hurricane Boundary Layer by Large Eddies. *Journal of Geophysical Research*, **113**, D17104, 2008.

Zhu, P., Menelaou, K. and Zhu, Z.: Impact of Subgrid-Scale Vertical Turbulent Mixing on Eyewall Asymmetric Structures and Mesovortices of Hurricanes: Impact of SGS Vertical Turbulent Mixing on Eyewall Asymmetries. *Quarterly Journal of the Royal Meteorological Society*, **140**, 416–438, 2013.

Table caption

Table 1 List of the identified tornado-scale vortices in the TCBL with the maximum updraft (m s^{-1}) and vertical relative vorticity (s^{-1}) and the corresponding altitudes (m) in the parentheses. The location column lists the radial distance from the TC center and the relative distance to the 500-m radius of maximum wind in the parentheses. The Richardson number (Ri) is averaged over the layer between 200-800 m within a radius of 1.5 km. The four strongest EVMs are indicated in bold.

Figure captions

Figure 1 Intensity of the simulated tropical cyclone during 24-36 h in terms of maximum instantaneous (red) and azimuthal-mean (blue) wind speeds at 10 m.

Figure 2 Simulated radar reflectivity (dBZ) at 500 m (a) and wind speed (m s^{-1}) at 10 m (b) within an area of 40×40 km^2 at 27 h. The plus signs and solid circles indicate the TC center and the radius of maximum wind at 500 m. The red dots indicate locations of tornado-scale vortices. The rectangle shows the area used in Fig. 3a. The arrow shows the vertical wind shear of 7.0 (27h) m s^{-1} between 200 hPa and 850 hPa.

Figure 3 (a) 10-m wind speed (m s^{-1}) and wind vectors and (b) the perturbation wind vectors and vertical component of relative vorticity (shading) at 500 m in the area shown in Fig. 2b. The straight line is the location of the vertical cross section in Figure 7 and M2701 and M2705 are the two tornado-scale vortices in the small area. The blue dots indicate their locations.

Figure 4 (a) Horizontal distribution of the tornado-scale vortices identified with the thresholds of 15 m s^{-1} (yellow dots) and 20 m s^{-1} (red dots) in vertical motion and the Richardson number (shading) averaged over 26-36 h; (b) the same as (a), but for 27 h. The solid circle is the 500-m radius of maximum wind and dashed circles indicate the distances from the TC center at 10-km intervals.

Figure 5 Radial-height cross sections of (a) tangential (shading) and radial (contour, interval: 2 m s^{-1}) wind speeds, (b) upward motion (contour, interval: 0.5 m s^{-1}) and radar reflectivity (shading), and (c) tangential wind (contour, interval: 4 ms^{-1}) and the vertical component of relative vorticity (shading, unit: s^{-1}), which are averaged over the northeastern quadrant during 26 h-36 h. The dots are the locations of identified tornado-scale vortices. The dashed white lines indicate the radius of maximum wind. The vertical and horizontal axes indicate the altitude (km) from the surface and the relative distances (km) from the TC center.

Figure 6 (a) The streamlines of the horizontal perturbation winds for M2701 and the wind speed (shading) at the altitude of 10 m. (b) The nearly vertical slice of the perturbation winds for M2701 with the red cycle indicating the updraft/downdraft couplet. (c) The stream lines of the three dimensional perturbation wind for M2701. The warm (cold) color of the streamline indicates the upward (downward) vertical velocity perturbation and the vectors show the near-surface wind fields. The vertical and horizontal axes indicate the altitude (km) from the surface and the relative distances (km) from the nearest corner, respectively.

Figure 7 The radial-height cross sections of the perturbation winds (vector) and (a) vertical motion, (b) equivalent potential temperature, and (c) radar reflectivity (shading) for M2701 along the line in Figure 3b. The abscissa indicates the relative outward distance.

Figure 8 (a) The radial-height cross section of perturbation winds (vector) and relative humidity (shading) for M2701, (b) the 400-m (blue) and 10-m (black) wind speeds and the 400-m vertical relative vorticity for M2701 along the line in Figure 3b. The abscissa indicates the relative outward distance.

Figure 9 The radial-height cross sections of the perturbation winds (vector) and (a) vertical motion, (b) equivalent potential temperature for M2708, and (c) the corresponding 900-m (blue) and 10-m (black) wind speeds. The abscissa indicates the relative outward distance.

Figure 10 The radial-height cross sections of the perturbation winds (vector) and (a) vertical motion, (b) equivalent potential temperature for M3002, and (c) the corresponding 1300-m (blue) and 10-m (black) wind speeds. The abscissa indicates the relative outward distance.

Table 2 List of the identified tornado-scale vortices in the TCBL with the maximum updraft (m s^{-1}) and vertical relative vorticity (s^{-1}) and the corresponding altitudes (m) in the parentheses. The location column lists the radial distance from the TC center and the relative distance to the 500-m radius of maximum wind in the parentheses. The Richardson number (Ri) is averaged over the layer between 200-800 m within a radius of 1.5 km. The four strongest EVMs are indicated in bold.

No.	Updraft	Vorticity	Location	Ri
M2600	22.75(800)	0.36(400)	23.6 (-5.5)	0.095
M2601	22.39(600)	0.23(500)	25.3 (-3.8)	0.111
M2700	27.37(500)	0.45(200)	25.6 (-3.0)	0.017
M2701	**31.98(400)**	**0.55(200)**	**24.3 (-4.3)**	**-0.008**
M2702	21.40(300)	0.30(300)	21.1 (-7.5)	0.029
M2703	20.46(400)	0.23(400)	27.9 (-0.7)	0.013
M2704	27.76(500)	0.34(400)	22.8 (-5.8)	0.032
M2705	22.26(600)	0.24(600)	27.9 (-0.7)	0.038
M2706	20.93(600)	0.23(500)	20.7 (-7.9)	-0.031
M2707	20.30(700)	0.21(700)	29.6 (1.0)	-0.011
M2708	22.20(900)	0.29(800)	31.2 (2.6)	-0.037
M2709	21.49(800)	0.22(800)	22.8 (-5.8)	0.052
M2800	20.12(400)	0.23(400)	27.0 (-1.7)	0.030
M2801	24.36(600)	0.39(400)	24.2 (-4.5)	-0.037
M2802	22.14(600)	0.30(500)	29.0 (0.3)	0.029
M2803	20.14(500)	0.23(500)	26.6 (-2.1)	0.025
M2900	**34.98(400)**	**0.48(200)**	**27.5 (-1.7)**	**0.042**
M2901	20.95(400)	0.21(400)	41.0 (11.8)	0.017
M3000	**35.77(400)**	**0.48(300)**	**28.1 (-0.1)**	**0.044**
M3001	**38.33(900)**	**0.49(400)**	**27.7 (-0.5)**	**0.067**
M3002	21.43(1300)	0.29(1300)	29.8 (1.6)	0.083
M3100	20.87(600)	0.24(700)	25.1 (-3.3)	-0.106
M3600	22.00(400)	0.35(400)	24.1 (-6.6)	0.146
M3601	22.68(600)	0.23(500)	38.0 (7.3)	-0.073

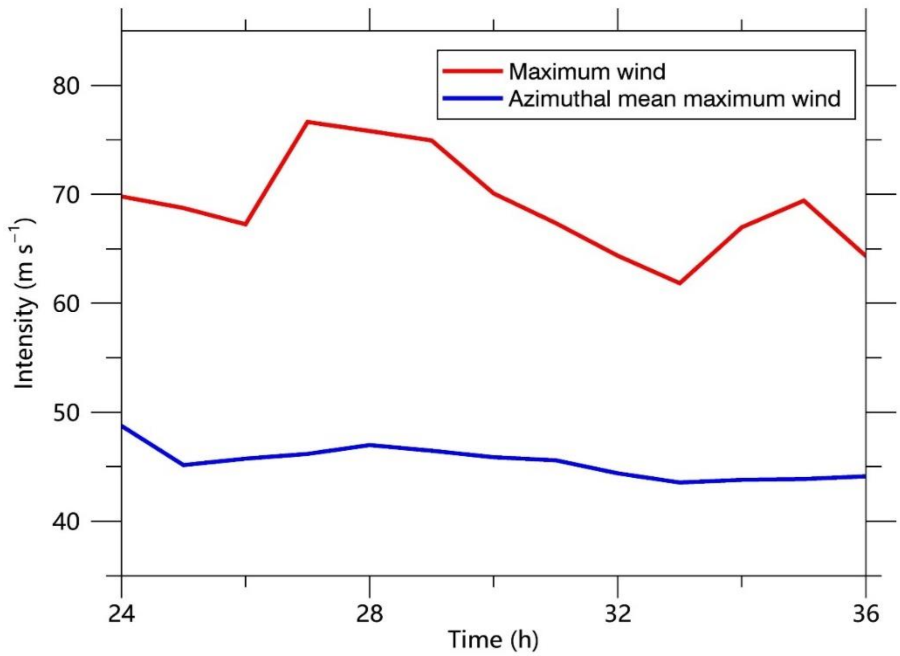

Figure 1 Intensity of the simulated tropical cyclone during 24-36 h in terms of maximum instantaneous (red) and azimuthal-mean (blue) wind speeds at 10 m.

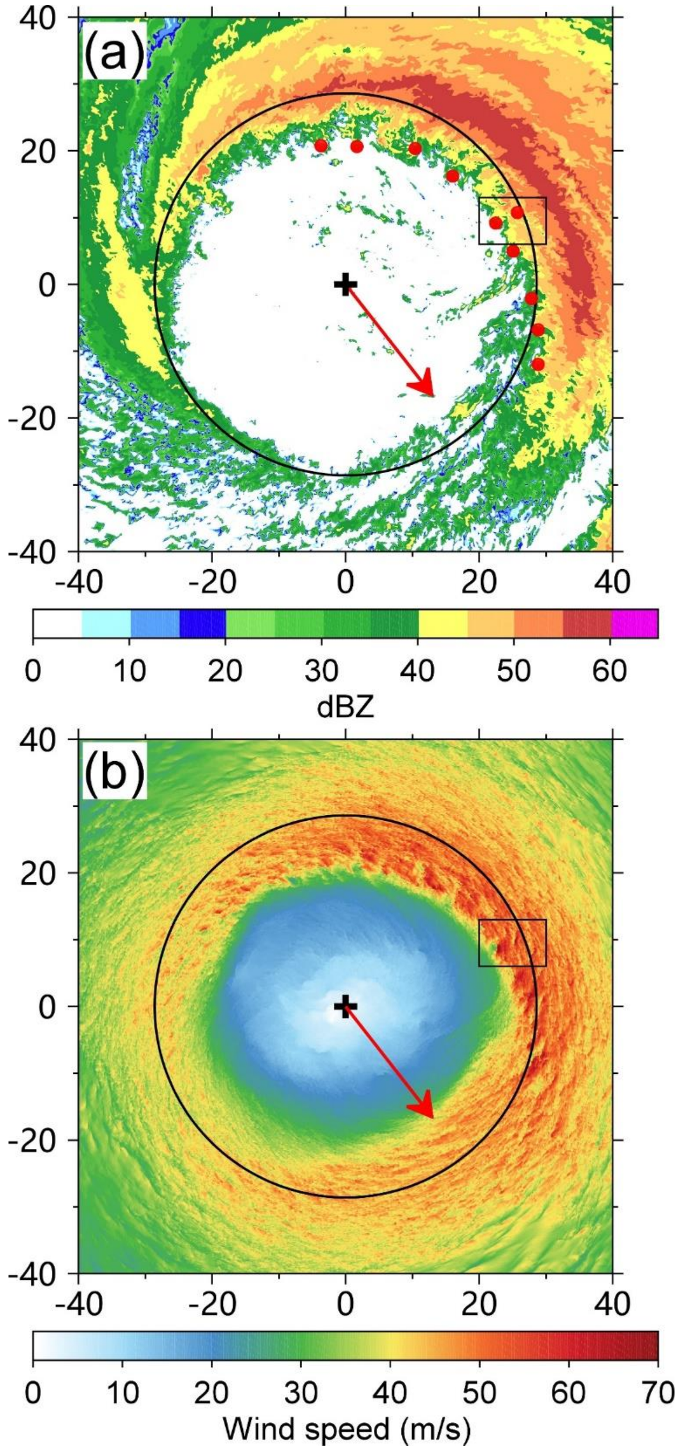

Figure 2 Simulated radar reflectivity (dBZ) at 500 m (a) and wind speed (m s^{-1}) at 10 m (b) within an area of 40×40 km^2 at 27 h. The plus signs and solid circles indicate the TC center and the radius of maximum wind at 500 m. The red dots indicate locations of tornado-scale vortices. The rectangle shows the area used in Fig. 3a. The arrow shows the vertical wind shear of 7.0 (27h) m s^{-1} between 200 hPa and 850 hPa.

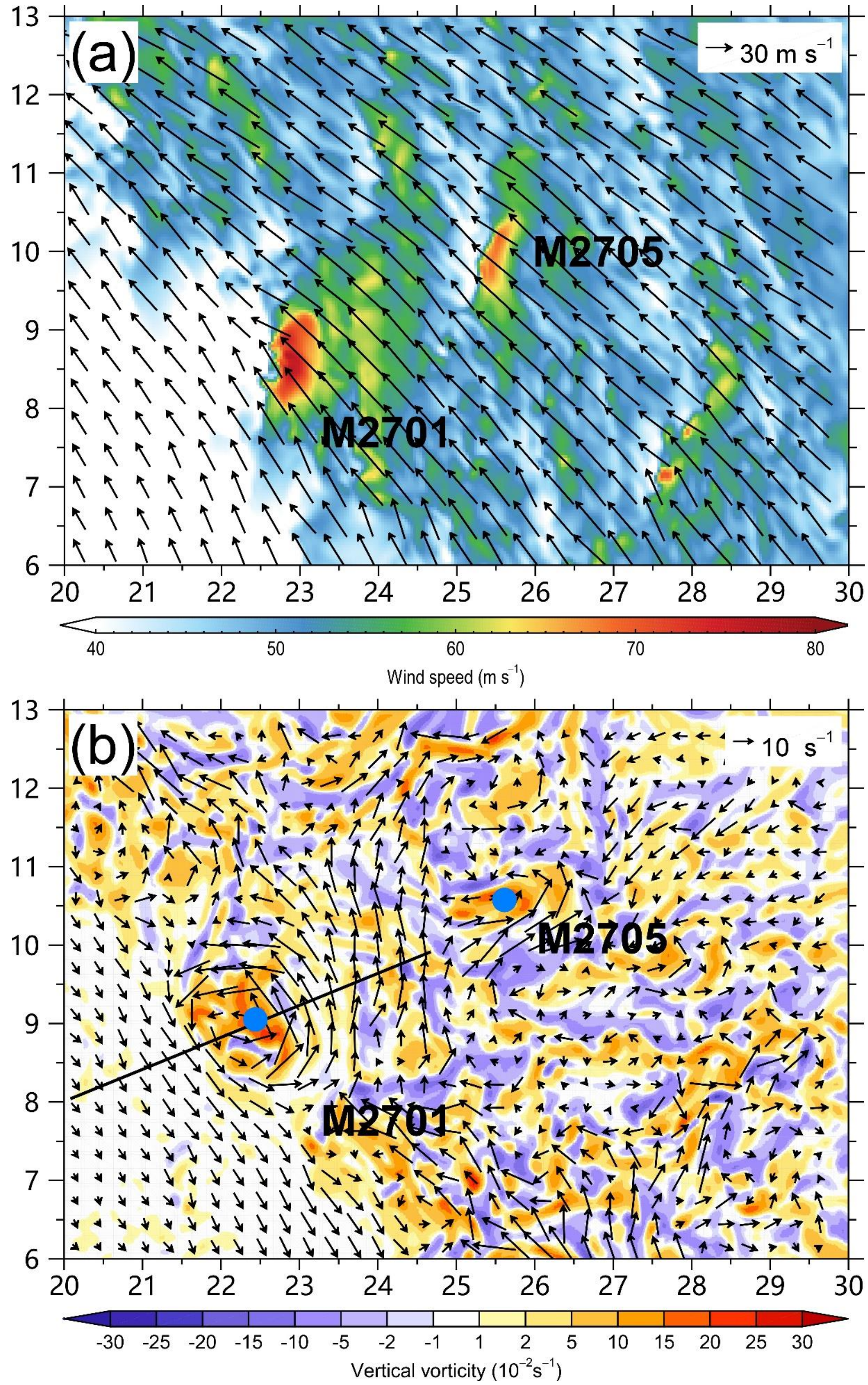

Figure 3 (a) 10-m wind speed (m s^{-1}) and wind vectors and (b) the perturbation wind vectors and vertical component of relative vorticity (shading) at 500 m in the area shown in Fig. 2b. The straight line is the location of the vertical cross section in Figure 7 and M2701 and M2705 are the two tornado-scale vortices in the small area. The blue dots indicate their locations.

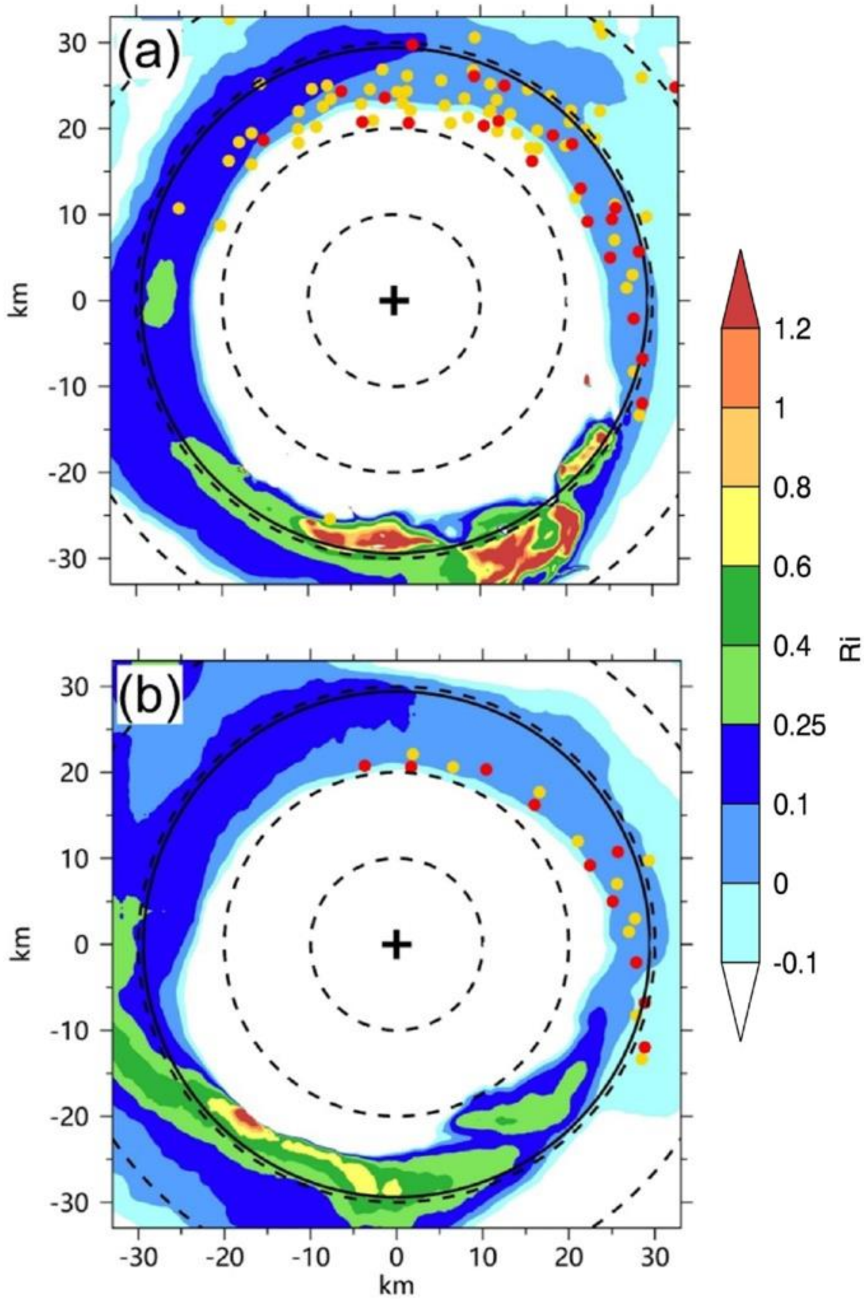

Figure 4 (a) Horizontal distribution of the tornado-scale vortices identified with the thresholds of 15 m s^{-1} (yellow dots) and 20 m s^{-1} (red dots) in vertical motion and the Richardson number (shading) averaged over 26-36 h; (b) the same as (a), but for 27 h. The solid circle is the 500-m radius of maximum wind and dashed circles indicate the distances from the TC center at 10-km intervals.

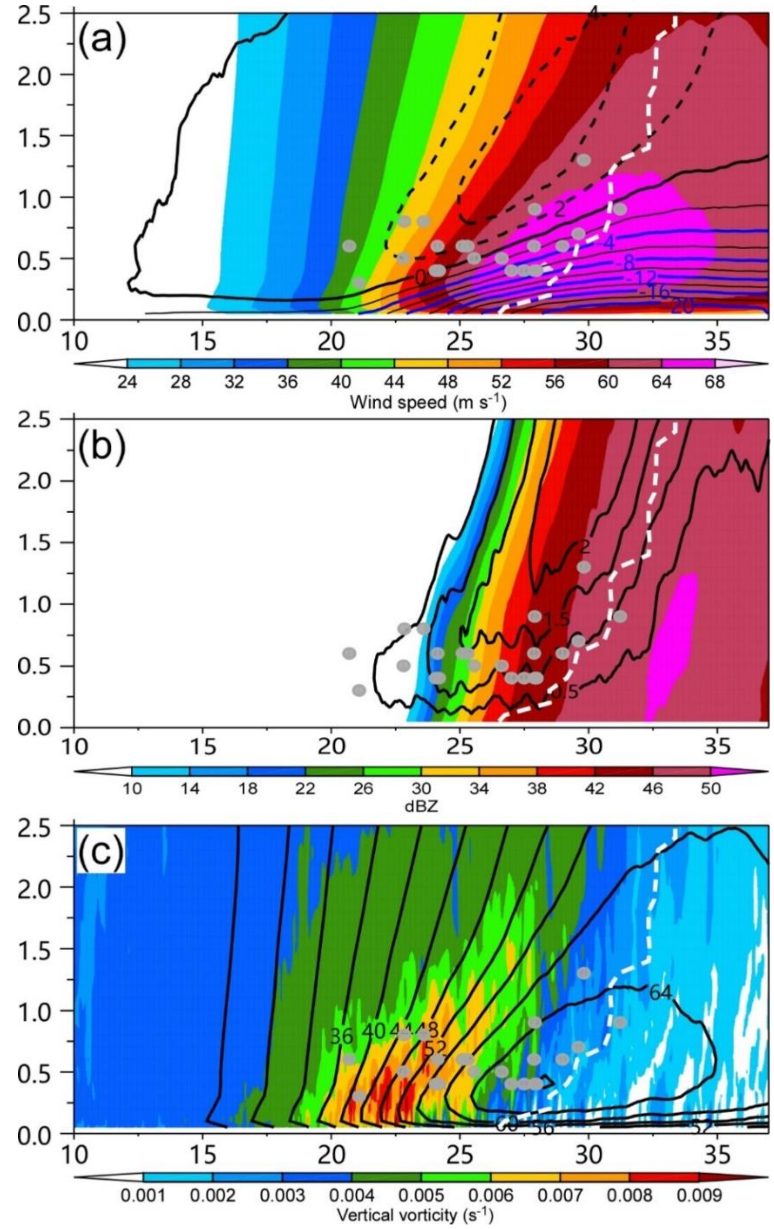

Figure 5 Radial-height cross sections of (a) tangential (shading) and radial (contour, interval: 2 m s^{-1}) wind speeds, (b) upward motion (contour, interval: 0.5 m s^{-1}) and radar reflectivity (shading), and (c) tangential wind (contour, interval: 4 ms^{-1}) and the vertical component of relative vorticity (shading, unit: s^{-1}), which are averaged over the northeastern quadrant during 26 h-36 h. The dots are the locations of identified tornado-scale vortices. The dashed white lines indicate the radius of maximum wind. The vertical and horizontal axes indicate the altitude (km) from the surface and the relative distances (km) from the TC center.

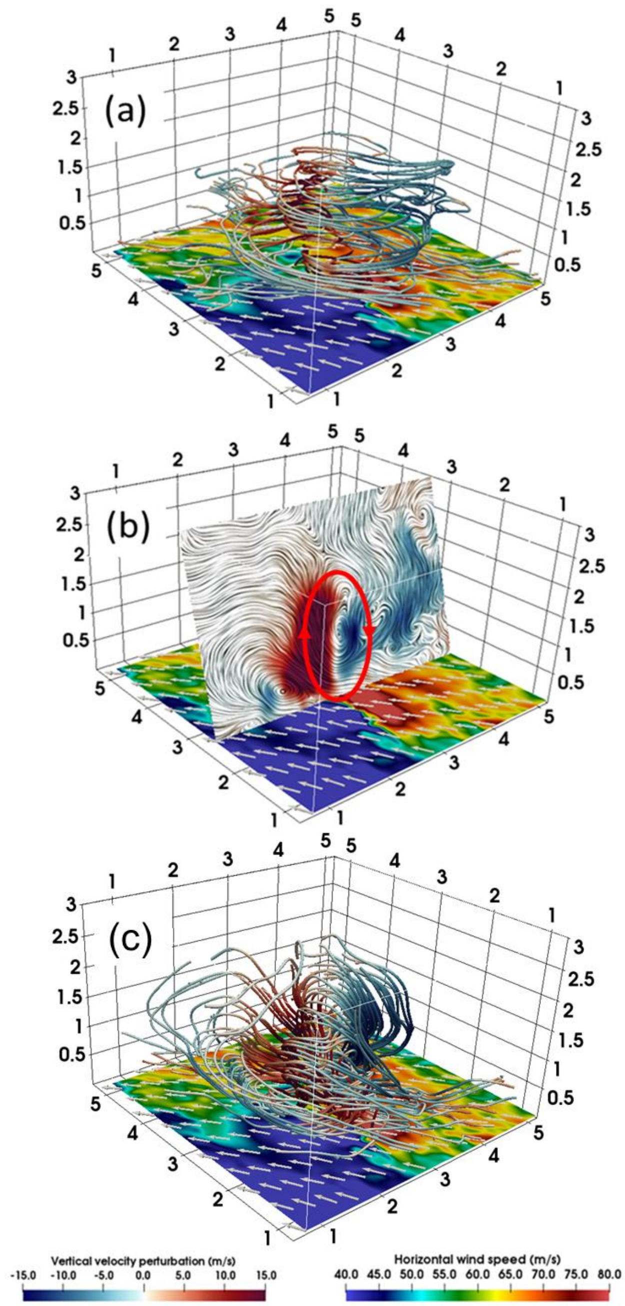

Figure 6 (a) The streamlines of the horizontal perturbation winds for M2701 and the wind speed (shading) at the altitude of 10 m. (b) The nearly vertical slice of the perturbation winds for M2701 with the red cycle indicating the updraft/downdraft couplet. (c) The stream lines of the three dimensional perturbation wind for M2701. The warm (cold) color of the streamline indicates the upward (downward) vertical velocity perturbation and the vectors show the near-surface wind fields. The vertical and horizontal axes indicate the altitude (km) from the surface and the relative distances (km) from the nearest corner, respectively.

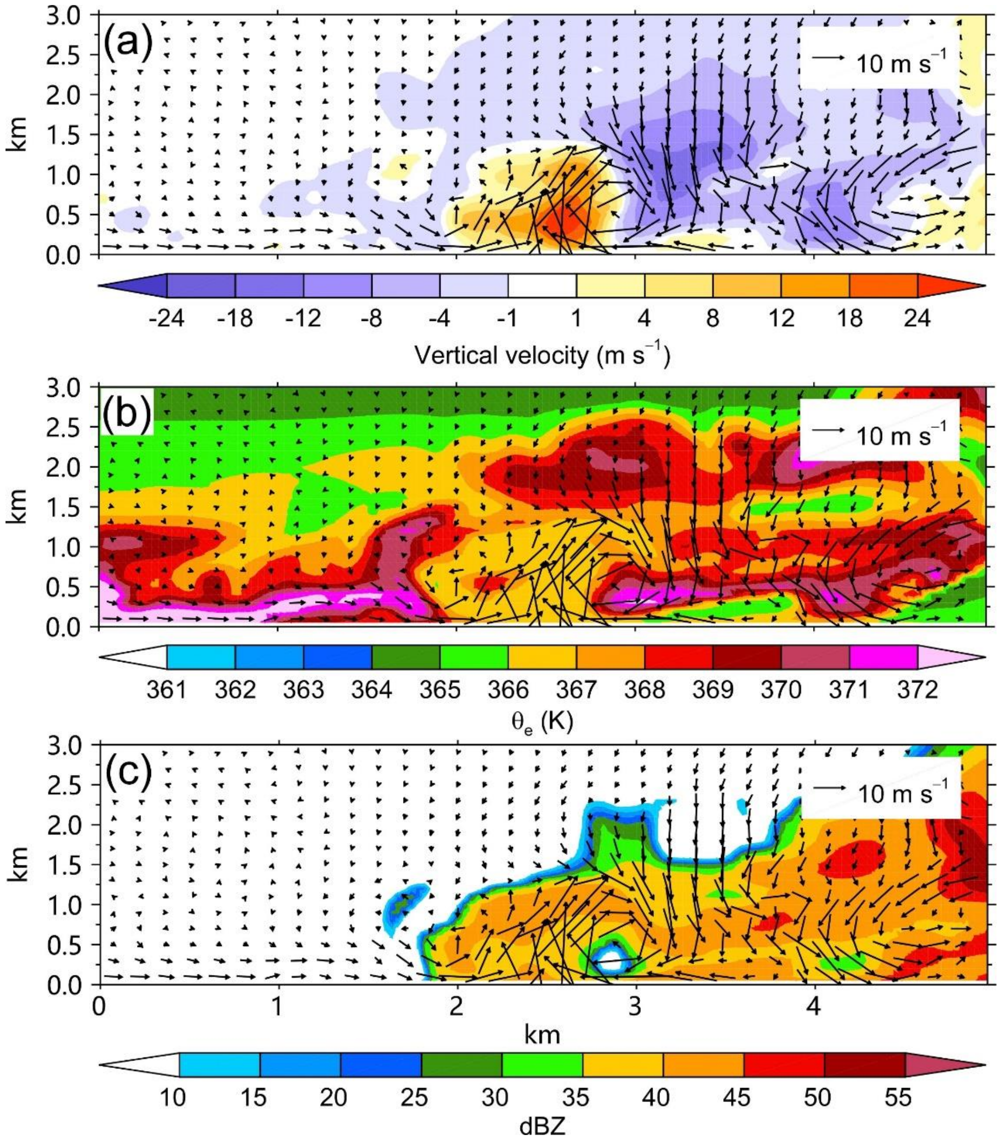

Figure 7 The radial-height cross sections of the perturbation winds (vector) and (a) vertical motion, (b) equivalent potential temperature, and (c) radar reflectivity (shading) for M2701 along the line in Figure 3b. The abscissa indicates the relative outward distance.

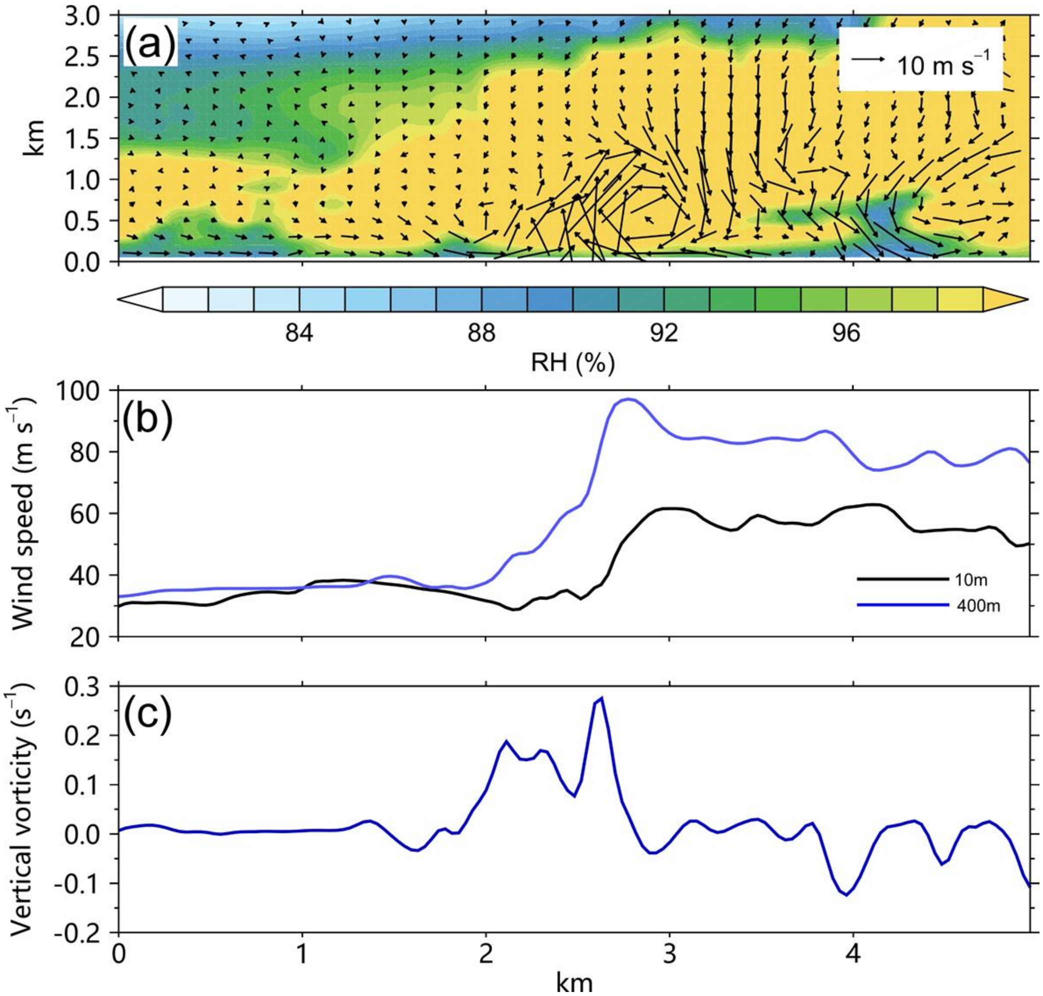

Figure 8 (a) The radial-height cross section of perturbation winds (vector) and relative humidity (shading) for M2701, (b) the 400-m (blue) and 10-m (black) wind speeds and the 400-m vertical relative vorticity for M2701 along the line in Figure 3b. The abscissa indicates the relative outward distance.

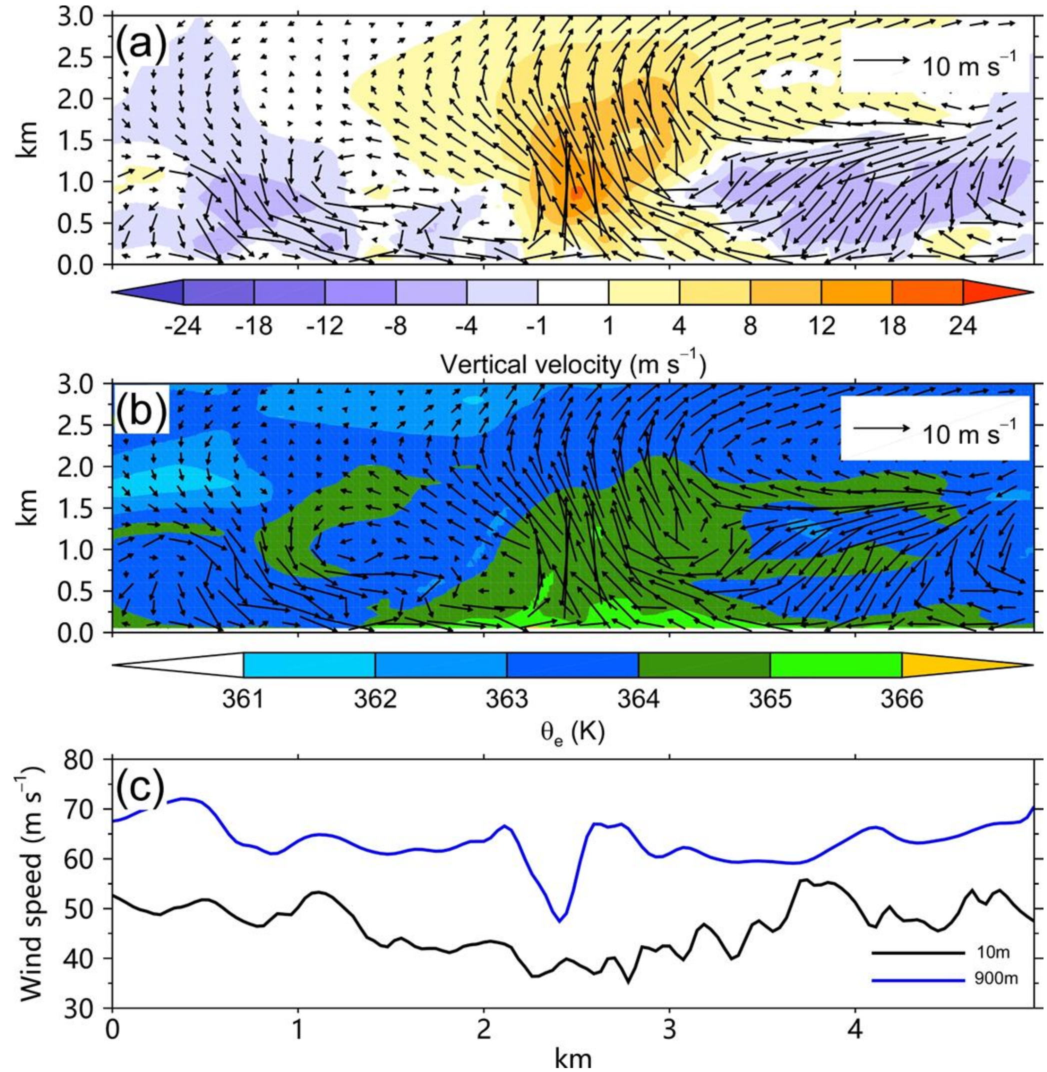

Figure 9 The radial-height cross sections of the perturbation winds (vector) and (a) vertical motion, (b) equivalent potential temperature for M2708, and (c) the corresponding 900-m (blue) and 10-m (black) wind speeds. The abscissa indicates the relative outward distance.

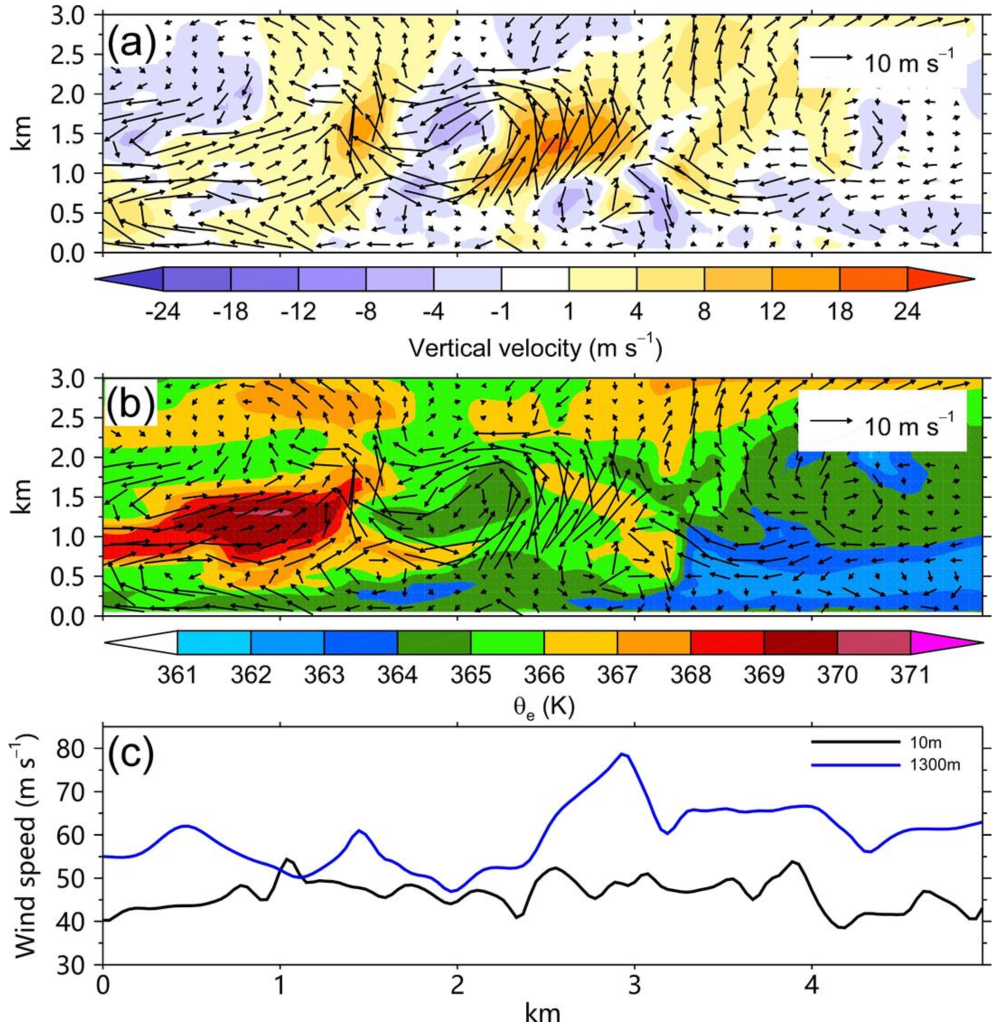

Figure 10 The radial-height cross sections of the perturbation winds (vector) and (a) vertical motion, (b) equivalent potential temperature for M3002, and (c) the corresponding 1300-m (blue) and 10-m (black) wind speeds. The abscissa indicates the relative outward distance.